Inorganic Chemistry

pubs.acs.org/IC Article

Catechol-Based Functionalizable Ligands for Gallium-68 Positron Emission Tomography Imaging

M. Andrey Joaqui-Joaqui, Mukesh K. Pandey,* Aditya Bansal, Mandapati V. Ramakrishnam Raju, Fiona Armstrong-Pavlik, Ayca Dundar, Henry L. Wong, Timothy R. DeGrado,* and Valérie C. Pierre*

Cite This: https://dx.doi.org/10.1021/acs.inorgchem.0c00975 Read Online

ABSTRACT: Four tris-bidentate catecholamide (CAM) ligands were synthesized, characterized, and evaluated as ligands for radiolabeling of gallium-68 for positron emission tomography (PET). Three of those ligands, 2,2-Glu-CAM, 3,3-Glu-CAM, and TREN-bisGlyGlu-CAM, incorporate ligand caps that contain a pendant carboxylic group for further conjugation to targeting moieties. The acyclic ligands all exhibited high (>80%) radiolabeling yields after short reaction times (<10 min) at room temperature, a distinct advantage over macrocyclic analogues that display slower kinetics. The stabilities of the four Ga^{III} complexes are comparable to or higher than those of other acyclic ligands used for gallium-68 PET imaging, such as desferrioxamine, with pGa values ranging from 21 to >24, although the functionalizable ligands are less stable than the parent Ga^{III}-TREN-CAM. *In vivo* imaging studies and *ex vivo* pharmacokinetic and biodistribution studies indicate that the parent [^{68}Ga]Ga-TREN-CAM is stable *in vivo* but is rapidly cleared in <15 min, probably via a renal pathway. The rapid and mild radiolabeling conditions, high radiolabeling yields, and high stability in human serum (>95%) render TREN-bisGlyGlu-CAM a promising candidate for gallium-68 chelation.

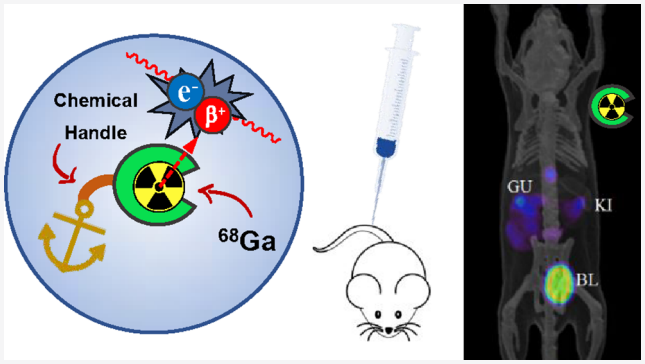

■ INTRODUCTION

Positron emission tomography (PET) is a standard and powerful imaging modality favored in the medical field for diagnosis and for evaluation of therapeutic methods due to its high sensitivity and its non-invasive nature.[1,2] Tracers used in PET imaging employ positron (β^+)-emitting radionuclides. Detection of the γ-rays emitted upon collision of the positrons (β^+) with nearby electrons (β^-) enables the spatial reconstruction of the tracer's distribution *in vivo*.[3] Two different approaches are pursued in the design of radiopharmaceutical imaging agents. The first involves organic molecules, often based on drugs, which incorporate a nonmetal PET radionuclide such as ^{11}C, ^{13}N, ^{15}O, or ^{18}F.[3−7] The second approach employs PET radioactive metals tightly coordinated by a chelate and often conjugated to a targeting moiety such as an antibody.[8,9] Among the metallic radionuclides employed for PET imaging, gallium-68 stands out as an attractive choice due to its convenient decay profile (mean β^+ energy of 0.89 MeV; $t_{1/2}$ = 68 min) and high positron yield (89%), which allow for sufficient levels of radioactivity for the production of high-quality images while minimizing the exposure of patients to a prolonged large and damaging dose of radiation.[3]

Past gallium-68 radiopharmaceuticals often employed chelators such as 1,4,7,10-tetraazacyclododecane-1,4,7,10-tetraacetic acid [DOTA (Figure 1)] because such macrocyclic ligands yield kinetically inert complexes while providing functional groups that are suitable for further conjugation to antibodies or other targeting moieties.[10] Examples used clinically include [^{68}Ga]Ga-DOTA^0-1Nal^{3}octreotide (DOTA-NOC), [^{68}Ga]Ga-DOTA^0-Tyr^{3}octreotide (DOTA-TOC), and [^{68}Ga]Ga-DOTA^0-Tyr^{3}octreotate (DOTA-TATE), three tracers that target somatostatin receptors that are overexpressed in neuroendocrine tumors (Figure 1).[11−14] Unfortunately, the high kinetic inertness of DOTA-based gallium complexes that advantageously slows dechelation and transmetalation to a time many-fold greater than the half-life of gallium-68 also imposes harsh reaction conditions for the formation of the complex. With such macrocyclic ligands, high temperatures, low pHs, and long reaction times (e.g., 90 °C, pH 3−5, and 30 min, respectively) are typically required to reach adequate radiolabeling yields.[15−19] Although such harsh conditions can be used with many peptide conjugates, they are incompatible with many targeting antibodies. Moreover, much of the

Received: April 1, 2020

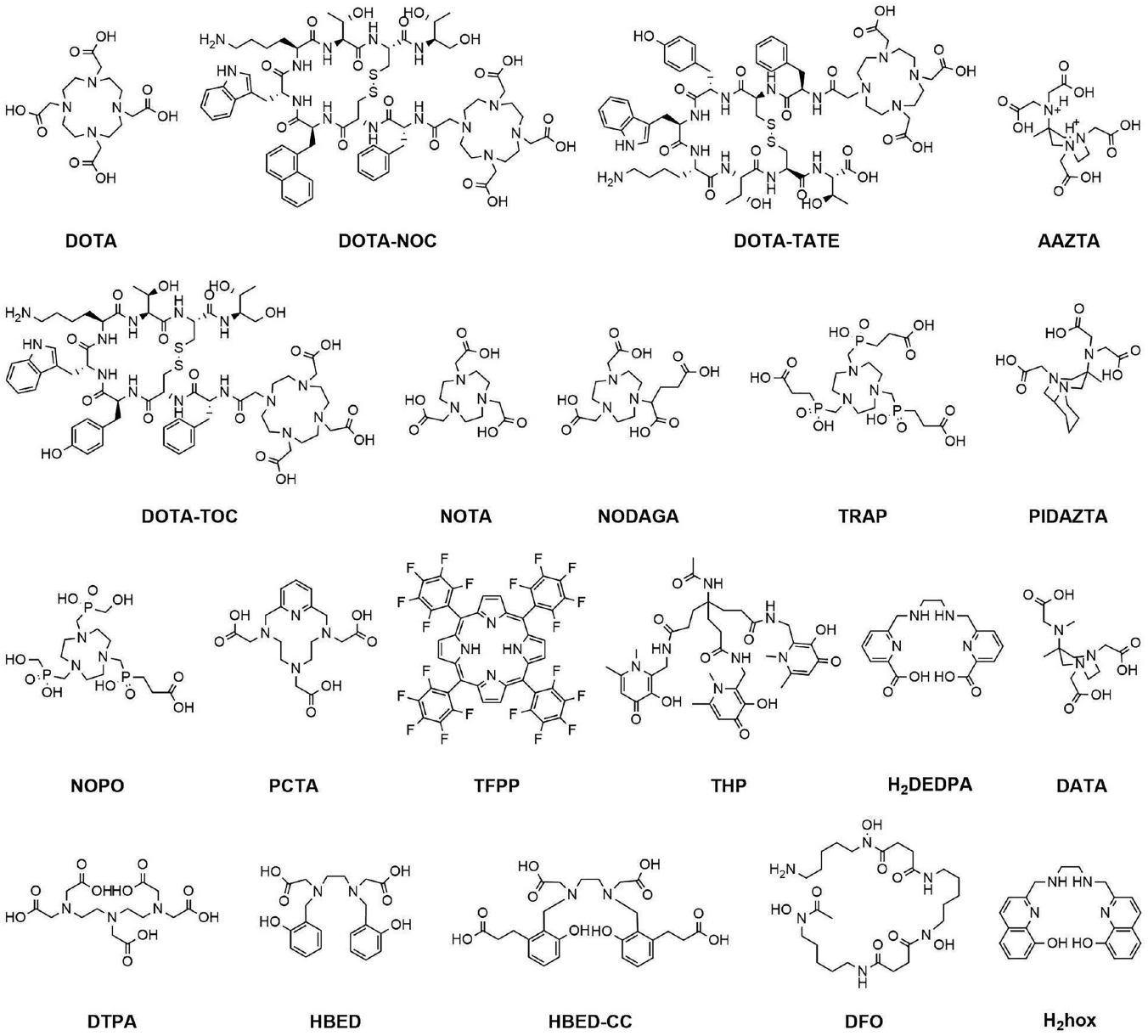

Figure 1. Structures of some common cyclic and acyclic chelators used for gallium-68 PET.

radioactivity of gallium-68 decays during the long reaction times needed for DOTA complexation. Such severe limitations led to the development of new chelators such as NOTA and NODAGA (Figure 1), whose smaller cages enable complexation of gallium-68 at room temperature in less time, typically <10 min.[20] However, complexation with these ligands still requires the use of acidic conditions that can be problematic with some targeting biomolecules. Similar drawbacks affect other macrocyclic ligands that have been reported (Figure 1), including TRAP,[21] NOPO,[22] PCTA,[23] and porphyrin scaffolds such as TFPP.[24]

Ultimately, for gallium-68 complexation to be performed efficiently and rapidly at room temperature and near-neutral pH, kinetically labile ligands must be used. Such ligands include acyclic or linear scaffolds such as DTPA [diethylenetriaminepentaacetatic acid (Figure 1)].[10] Unfortunately, the gallium complex of DTPA is not sufficiently thermodynamically stable to prevent dechelation and/or transmetalation *in vivo*.[25−27] Recent linear chelators with increased thermodynamic stability such as HBED-CC (Figure 1) have more potential.[28,29] Its prostate-specific membrane antigen conjugate, PSMA-HBED-CC, is currently one of the most widely used PET imaging agents.[30] Other ligands such as THP[10] and H_2DEDPA,[31] AAZTA,[32] DATA,[33] PIDAZTA,[34] and the recently reported H_2hox[35] are also promising chelating moieties for gallium-68 PET imaging.

Despite the potential of these recent gallium-68 chelators, there remains a need for new compounds that enable radiolabeling to be performed with high yields, rapidly, at room temperature and near-physiological pH. The further development of such chelators into radiopharmaceuticals requires that the chelate contain a pendant functional group for further conjugation to targeting biomolecules. High thermodynamic stability, which is necessary for kinetically labile radiolabels to be successful *in vivo*, can be achieved by matching the coordination number, geometry, cavity size, and chelating functionality to those favored by gallium(III). Given the similarity in coordination chemistry between Ga^{3+} and Fe^{3+}

https://dx.doi.org/10.1021/acs.inorgchem.0c00975
Inorg. Chem. XXXX, XXX, XXX−XXX

ions, those requirements have led researchers to explore the potential of chelators historically developed and optimized for iron as templates for ^{68}Ga-labeled radiopharmaceuticals.[36] In particular, siderophores, which are low-molecular weight natural product iron chelators secreted by bacteria and fungi specifically for Fe^{3+} chelation, are promising scaffolds.[37] The gallium-68 and gallium-67 complexes of desferrioxamine [DFO (Figure 1)], a hydroxamate-based bacterial siderophore, for instance, have been successfully used for PET imaging.[38] Advantageously, targeting moieties can be conjugated to DFO via its N-terminus, as in the tumor-targeting [^{67}Ga]Ga-DFO-succinyl-D-Phe-octreotide.[39] Unfortunately, because they are not sufficiently strong chelators, DFO conjugates have been reported to leach the radionuclide *in vivo*.[40−42] Similarly, the ^{68}Ga complex of pyoverdine, a mixed type siderophore from *Pseudomonas* species with both catecholate and hydroxamate coordinating moieties, has also shown potential for imaging some bacterial infections by PET.[43] However, pyoverdine lacks a pendant functional group for further bioconjugation, which limits its use for targeted imaging.

Enterobactin (Figure 2), a siderophore produced by most members of the Enterobacteriaceae family, is one of the most powerful siderophores due to its three preorganized catechol moieties. Accordingly, its pFe value, 35.5,[44] where pFe is defined as

$$\mathrm{pFe} = -\log[\mathrm{Fe}]_{\mathrm{free}} \text{ when } [\text{enterobactin}]_{\mathrm{total}} = 10^{-5}\ \mathrm{M} \text{ and } [\mathrm{Fe}]_{\mathrm{total}} = 10^{-6}\ \mathrm{M} \quad (1)$$

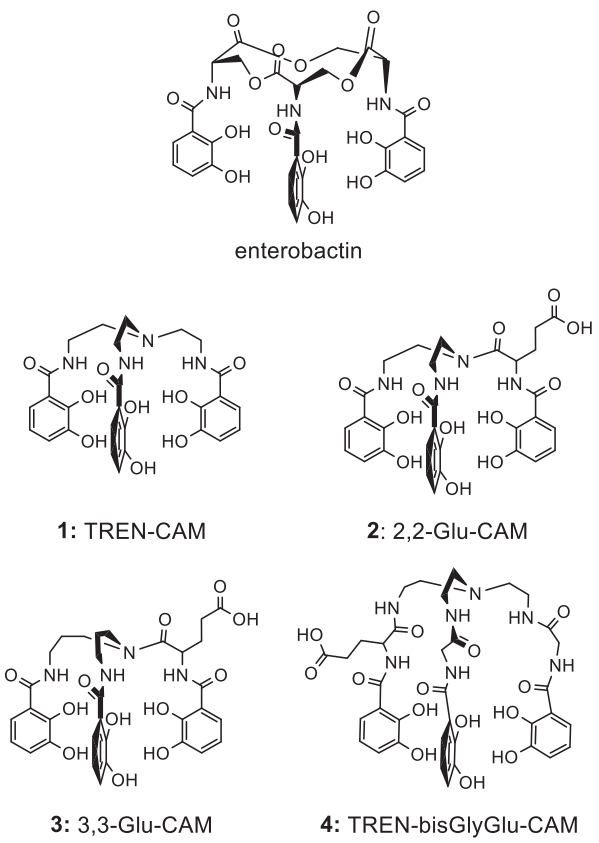

Figure 2. Chemical structures of functionalizable enterobactin-based PET ligands.

is one of the highest known for iron(III) complexes (the higher the pM value, the more stable the complex). The $^{67}Ga^{III}$ complex of enterobactin has also been reported.[45,46] Enterobactin has, however, not been evaluated for gallium-68 complexation and further application in PET imaging. There are a number of reasons why it would be a poor choice as a gallium-68 chelator for *in vivo* imaging applications. First, it lacks a chemical handle for further conjugation of a targeting moiety. Second, the trilactone backbone is prone to hydrolysis under physiological conditions, which would render the ^{68}Ga complex unstable *in vivo*.[44]

With this in mind, and to expand the toolkit of molecular radiotracers, we aim to apply the literature on enterobactin mimics for iron(III) coordination to the development of novel ligands for ^{68}Ga.[45,47,48] Specifically, we sought to design, synthesize, and evaluate new ligands that could chelate [^{68}Ga]Ga^{3+} rapidly under mild conditions at physiological pH and room temperature with high radiochemical yields and would be thermodynamically stable as needed for *in vivo* applications. To avoid the problem of the propensity of lactones toward hydrolysis, the backbone of enterobactin was replaced in our four ligands with more stable amines and amide caps (Figure 2). As with enterobactin, all four ligands are tripodal and contain three catecholate coordinating moieties (CAMs) as needed for strong coordination of the metal ion.[49] Three of the ligands, 2,2-Glu-CAM (**2**), 3,3-Glu-CAM (**3**), and TREN-bisGlyGlu-CAM (**4**), also contain pendant carboxylic acid functional groups that enable further bioconjugation. Those four ligands differ in the size of their chelating cavity, which is expected to influence both radiolabeling yield and thermodynamic stability.

RESULTS AND DISCUSSION

Synthesis. The synthesis of the tripodal enterobactin analogue TREN-CAM (**1**) was previously reported via a route that uses methyl-protected catechols and thus necessitates subsequent harsh deprotection conditions.[50] To use milder conditions, we have instead employed benzyl protecting groups and synthesized **1** according to Scheme 1. Benzyl-

Scheme 1. Synthesis of TREN-CAM (1)[a]

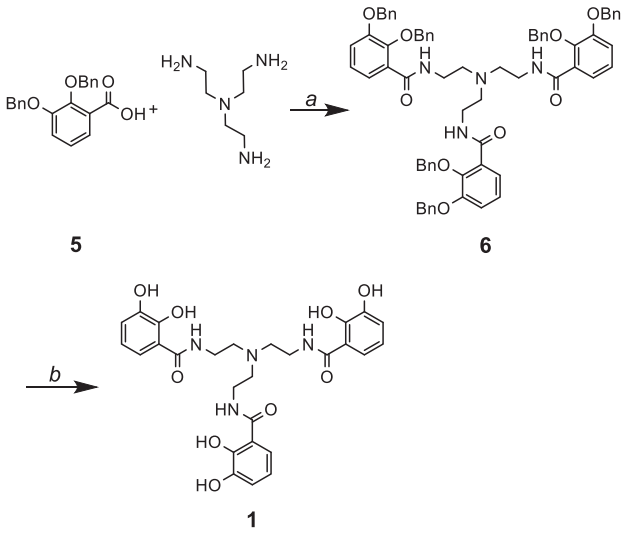

[a]Reagents and conditions: (a) TBTU, DIPEA, CH_2Cl_2, rt, 24 h; (b) HCl/AcOH, rt, 24 h.

https://dx.doi.org/10.1021/acs.inorgchem.0c00975
Inorg. Chem. XXXX, XXX, XXX−XXX

protected 2,3-dihydroxybenzoic acid (**5**) was synthesized in two steps from commercial sources as reported by Gardner et al.[51] The TREN-capped benzyl-protected tripodal ligand (**6**) was subsequently formed under standard coupling conditions with 2-(1*H*-benzotriazol-1-yl)-1,1,3,3-tetramethylaminium tetrafluoroborate (TBTU). Deprotection under acidic conditions yielded the final ligand TREN-CAM (**1**) that was stored under N_2(g) in the dark at 4 °C due to the susceptibility of catecholamides to oxidation.[52,53]

The ligands 2,2-Glu-CAM (**2**) and 3,3-Glu-CAM (**3**) were synthesized according to Scheme 2 starting from the

Scheme 2. Synthesis of 2,2-Glu-CAM (2) and 3,3-Glu-CAM (3)[a]

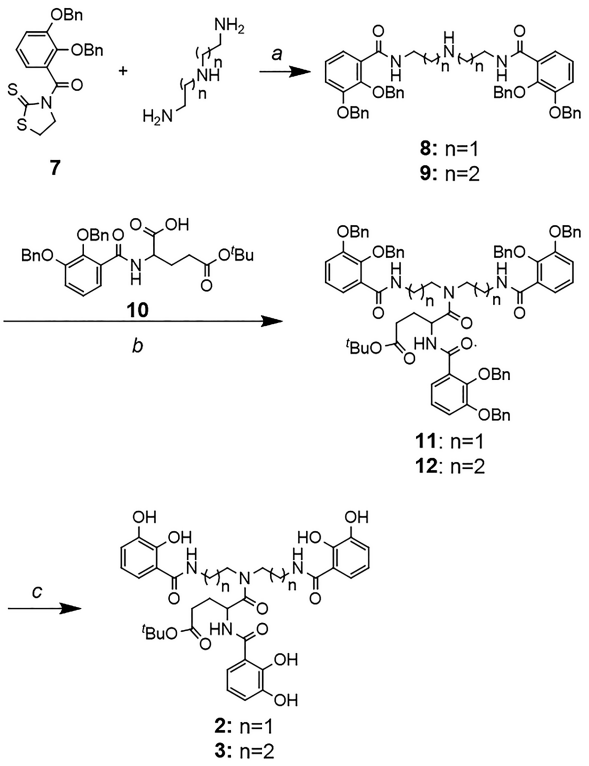

[a]Reagents and conditions: (a) CH_2Cl_2, rt, 48 h; (b) TBTU, DIPEA, CH_2Cl_2, rt, 24 h; (c) HCl/AcOH, rt, 30 h.

thiazolidine-activated intermediate CAM(Bn)thiaz (**7**) that was previously synthesized according to the procedure reported by Allred et al.[54] Advantageously, the thiazolidine activating group enables chemoselective coupling of the CAM moiety to the primary amines of the diethylenetriamine and dipropylenetriamine backbones to yield bis-amides **8** and **9**, respectively. Separately, Glu(^{t}Bu)-CAM(Bn) (**10**) was synthesized as reported by Dertz et al.[55] Conjugation of the arm **10** to intermediate **8** or **9** under standard coupling conditions with TBTU yielded the fully protected ligand 2,2-Glu(^{t}Bu)-CAM(Bn) (**11**) or 3,3-Glu(^{t}Bu)-CAM(Bn) (**12**), respectively. The *tert*-butyl and benzyl protecting groups were subsequently removed simultaneously under acidic conditions to yield the final ligands 2,2-Glu-CAM (**2**) and 3,3-Glu-CAM (**3**), both of which were kept under N_2(g) in the dark at 4 °C.

The final ligand, TREN-bisGlyGlu-CAM (**4**), was synthesized according to Scheme 3. In a first step, the benzyl-protected podand GlyCAM(Bn) (**14**) was synthesized in a

Scheme 3. Synthesis of TREN-bisGlyGlu-CAM (4)[a]

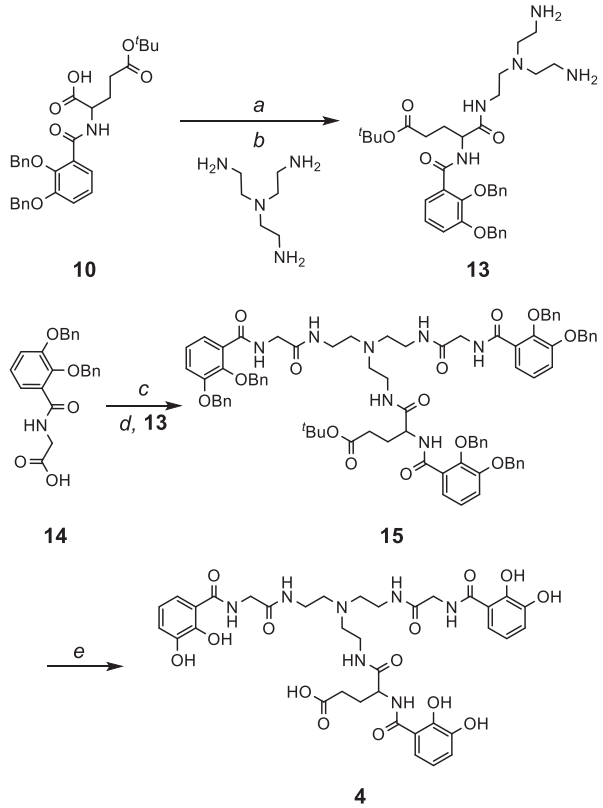

[a]Reagents and conditions: (a) NHS, EDC·HCl, 1,4-dioxane, 0 °C, 24 h; (b) DIPEA, 1,4-dioxane, rt, 30 h; (c) NHS, EDC·HCl, CH_2Cl_2, 0 °C, 24 h; (d) DIPEA, CH_2Cl_2, rt, 30 h; (e) HCl/AcOH, rt, 20 h.

manner similar to that of Glu(^{t}Bu)CAM(Bn) (**10**) according to the procedure of Dertz et al.[55] *In situ* *N*-hydroxysuccinimide (NHS) activation of the arm Glu(^{t}Bu)CAM(Bn) (**10**) with *N*-ethyl-*N*′-(3-dimethylaminopropyl)carbodiimide hydrochloride (EDC·HCl) enabled further conjugation to the tris(2-aminoethyl)amine backbone to yield the monosubstituted TREN intermediate **13**. *In situ* NHS activation of the second arm, GlyCAM(Bn) (**14**), enabled conjugation to the two remaining primary amines of **13** and completion of the fully protected ligand (**15**). Simultaneous deprotection of the *tert*-butyl and benzyl groups under acidic conditions yielded the final ligand **4** that was kept under N_2(g) in the dark at 4 °C.

Stability of Ga(III) Complexes. For labile $^{68}Ga^{III}$ complexes to be viable candidates for PET imaging, the complexes must be sufficiently stable so that the radioactive metal does not leach out of the agent and into undesired sites. Because it is the radionuclide metal ion that is imaged, any decomplexation would prevent accurate imaging of the desired targets. Achieving high stability is particularly important given the low concentration of PET agents used *in vivo*, concentrations that favor decomplexation.

The stability of metal complexes with differing numbers of protonation steps is best compared not by their formation constants but by their pM values, where $pM = -\log[M]_{free}$ (eq 1). For Ga^{3+} complexes, the relevant pM value is pGa. This thermodynamic parameter is typically reported under physiological pH (7.4) at [L] = 10 μM and [M] = 1 μM. Advantageously, unlike formation constants (K_a), pM values enable direct comparison of the complexation behavior of

https://dx.doi.org/10.1021/acs.inorgchem.0c00975
Inorg. Chem. XXXX, XXX, XXX−XXX

ligands that differ in basicity, protonation state, or even metal ion:ligand stoichiometry.[3] The larger the pGa value, the less free (uncomplexed) Ga^{3+} is present in solution, and the more stable the Ga^{3+} complex.

pM values can be calculated from the association constants of the metal complex and the protonation steps of both the free ligand and the metal complex. They can also be directly evaluated at a given pH by competition with a well-characterized ligand, without prior determination of the protonation constants.[56,57] DFO is a ligand whose Ga^{3+} complex is well characterized, which undergoes ligand exchange and reaches thermodynamic equilibrium rapidly, and which has previously been investigated for gallium-68 PET imaging; it is thus ideal for determining the stability of the catechol-based ligands **1**−**4**.[58] Competition titrations were performed as previously reported.[56,57] Ligand exchange was monitored by ultraviolet−visible spectroscopy after equilibration at 25 °C for 24 h. The results are shown in Figure 3. The concentration of competing DFO necessary to generate an equal partition of Ga^{3+} between the two ligands [log([DFO]/[L]) when log([Ga-DFO]/[Ga-L]) = 0] directly gives the difference in the pM value between the ligand of interest and DFO. Because the pGa for Ga-DFO is known (21.2 at pH 7.4 and 25 °C),[35] the pGa values of ligands **1**−**4** at the same pH and temperature can be directly calculated. It is noteworthy that because pM values are independent of the isotope of the metal ion, these experiments were performed with the naturally occurring and nonradioactive Ga isotope.

The results of the competition experiments are listed in Table 1. Notably, TREN-CAM forms such a stable Ga^{3+} complex that even a 1000-fold excess of DFO did not result in enough ligand exchange to be accurately measured. As such, a precise pGa value for Ga-TREN-CAM could not be determined, although a lower limit of 24, 3 units higher that of Ga-DFO (pGa = 21.2), can be conservatively estimated. Ga-TREN-CAM is thus one of the most stable Ga^{III} complexes evaluated for PET imaging. It is at least 1 and 6 orders of magnitude more stable than TRAP (pGa = 23.1) and DOTA (pGa = 18.5), respectively.[35]

The carboxylate-bearing ligands 2,2-Glu-CAM (**2**), 3,3-Glu-CAM (**3**), and TREN-bisGlyGlu-CAM (**4**) all form less stable Ga^{III} complexes than the parent TREN-CAM ligand. The stabilities of these three functionalizable complexes span nearly 2 orders of magnitude, with 2,2-Glu-CAM (**2**), which has the smallest ligand cap, being the most stable and TREN-bisGlyGlu-CAM (**4**), which has the largest ligand cap, being the least stable. A smaller cap is therefore preferred for the Ga^{3+} ion. The decrease in stability compared to that of the parent Ga-TREN-CAM could be due to a number of parameters. The tight hydrogen-bonding network of the ligand's TREN backbone that predisposes the ligand TREN-CAM and increases the stability of its metal complex is significantly altered in the other three ligand caps.[59] Previous work by our group and others on lanthanide and iron complexes previously reported such a decrease in the pM value upon modification of the TREN backbone.[55,59−61] Complex charge is also known to affect the stability of d^{10} metal ions that lack ligand field stabilization energy such as Ga^{III}.[57,62] The more negative the charge, the less stable the coordination complex. The pendant carboxylates of ligands **2**−**4**, which are deprotonated at neutral pH, thus likely also contribute to the decrease in the pGa value. Nonetheless, these ligands all form complexes that are more stable than many other ligands used

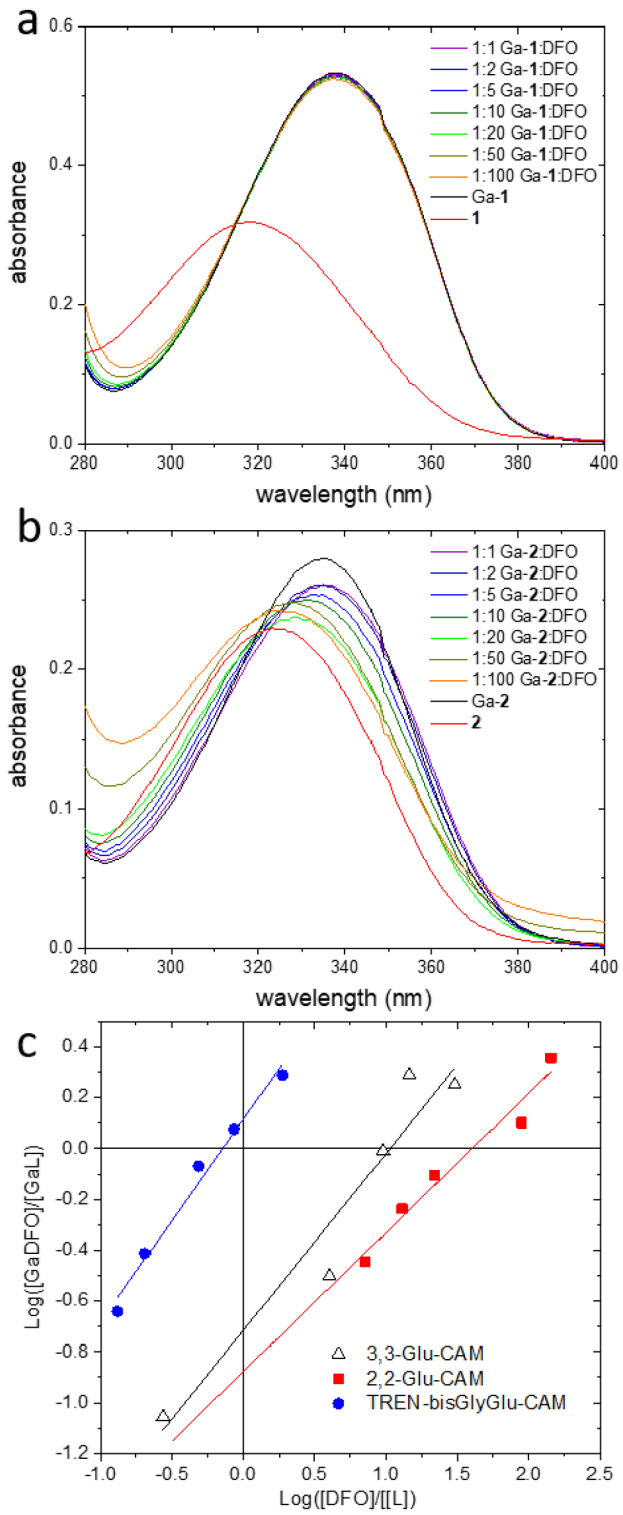

Figure 3. Competition of Ga^{III} complexes with DFO: (a) spectra of Ga^{III}-TREN-CAM upon addition of increasing concentrations of DFO, (b) spectra of Ga^{III}-2,2-Glu-CAM upon addition of increasing concentrations of DFO, and (c) competition titrations of functionalizable ligands **2**−**4** against DFO. The *x* intercepts indicate the difference in pGa between each catechol ligand and the competing DFO. Experimental conditions: 0.01 M TRIS buffer, pH 7.4, 0.1 M KCl, 25 °C.

https://dx.doi.org/10.1021/acs.inorgchem.0c00975
Inorg. Chem. XXXX, XXX, XXX−XXX

Table 1. pGa Values of Tris-catecholate Ga^{III} Complexes[a]

ligand	$pGa_L - pGa_{DFO}$	pGa
TREN-CAM (**1**)	>3	>24
2,2-Glu-CAM (**2**)	1.60	22.8
3,3-Glu-CAM (**3**)	1.03	22.2
TREN-bisGlyGlu-CAM (**4**)	−0.14	21.1
DFO[b]		21.2

[a]Experimental conditions: 0.01 M TRIS(aq), pH 7.4, 0.1 M KCl, 25 °C ([Ga^{3+}] = 1 μM, [DFO] = 10 μM, pH 7.4, and 25 °C). [b]From ref 35.

clinically for gallium-68 PET imaging, including DOTA. Additionally, ligands **1**−**4** have a higher affinity for Ga^{3+} than transferrin (pGa = 19.7),[63] a serum protein that is well-known for its capability to sequester Ga^{3+} ions, thereby leading to dechelation of weak gallium-68 agents *in vivo*.[64] While this is promising for *in vivo* use of ligands **1**−**4**, it is important to note that blood is a complex matrix that also contains other endogenous chelating species that could also lead to decomplexation of the gallium-68 tracers.

Gallium-68 Radiolabeling Yields. Though the thermodynamic stability of the Ga^{III} complexes is important, it is only one of the parameters that determines the viability of a chelator for PET imaging. Practically, a chelate must also be able to complex the radionuclide rapidly. Gallium-68, like ^{18}F ($t_{1/2}$ = 110 min), has a limited half-life ($t_{1/2}$ = 68 min), and thus, radiolabeling must be achieved efficiently and quickly, ideally in <10 min.[65] This short reaction time does not necessarily enable the system to reach thermodynamic equilibrium. Although thermodynamic values such as pGa give a good indication of the stability of a complex in complex biological media, they do not necessarily guarantee a high labeling yield if kinetics of complexation are slower than the reaction time.

Radiochemical labeling yields were determined for the four catechol-based ligands as depicted in Scheme 4. All experiments were performed under the same short reaction time, 10 min, at room temperature under slightly basic conditions. [^{68}Ga]$GaCl_3$ was produced via zinc-68 (p,n) gallium-68 nuclear reaction using a cyclotron in a liquid target and purified using hydroxamate resin as reported previously.[66,67] The results, given in Table 2, indicate that the ligand that forms the most stable Ga^{III} complex, TREN-CAM (**1**), also exhibits the highest radiolabeling yield, coordinating [^{68}Ga]-Ga^{3+} almost quantitatively in 10 min at room temperature. The three functionalizable catechol-based ligands **2**−**4** also enable high radiolabeling yields of >80% under short reaction times at room temperature. Though not quantitative, the measured radiolabeling levels are superior to the radiochemical yields reported for some DOTA bioconjugates such as DOTA-TOC and DOTA-NOC. However, the macrocyclic DOTA-based ligands, unlike the catecholates **1**−**4**, need to be subjected to high temperatures (90 °C) and acidic pH to reach such radiolabeling levels.[19] The catechol ligands **1**−**4** also compare positively to other acyclic chelators that are also labile and thus chelate gallium rapidly.[58] TREN-CAM (**1**), 2,2-Glu-CAM (**2**), and TREN-bisGlyGlu-CAM (**4**) all exhibit radiolabeling yields ≥90%, values that are typical of the more favored rapid chelators HBED, DFO, and THP (all ≥92%).[58]

Scheme 4. Radiolabeling of TREN-CAM with [^{68}Ga]$GaCl_3$

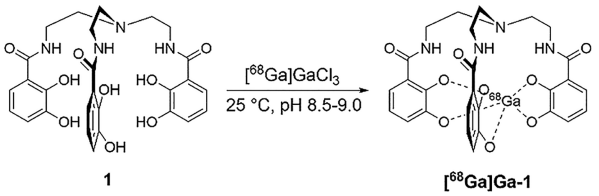

Table 2. Radiolabeling Conditions and Yields of Ligands

complex	yield (%)
TREN-CAM (**1**, n = 10)[a]	94 ± 6
2,2-Glu-CAM (**2**, n = 2)[a]	91 ± 4
3,3-Glu-CAM (**3**, n = 3)[a]	83 ± 6
TREN-bisGlyGlu-CAM (**4**, n = 2)[a]	90 ± 1
DFO[b]	96 ± 1
THP[b]	96 ± 1
HBED[b]	92 ± 1

[a]Labeling conditions for this work: T = 25 °C, pH 8.0−9.0, t = 10 min. Reaction volumes were 142 μL. The ligand concentrations used for radiolabeling were TRENCAM (213 μM), 2,2-Glu-CAM (185 μM), 3,3-Glu-CAM (177 μM), and TREN-bisGlyGlu-CAM (185 μM). [b]Labeling conditions from ref 58: 500 μM, T = 25 °C, pH 6.5, t = 10 min.

From Le Châtelier's principle, the formation of the Ga^{III} complex is favored under concentrated conditions and disfavored under diluted ones. The radiolabeling yield is thus highly dependent on the concentration of ligand and [^{68}Ga]$GaCl_3$ used. As shown in Figure 4 for the best chelator, TREN-CAM (**1**), the radiolabeling yield remains high but decreases sharply if the ligand concentration is <0.5 mM. This is a minimum ligand concentration that is slightly higher than those observed for DOTA, NOTA, and HBED, although gallium labeling with those ligands is typically performed under acidic conditions.[10]

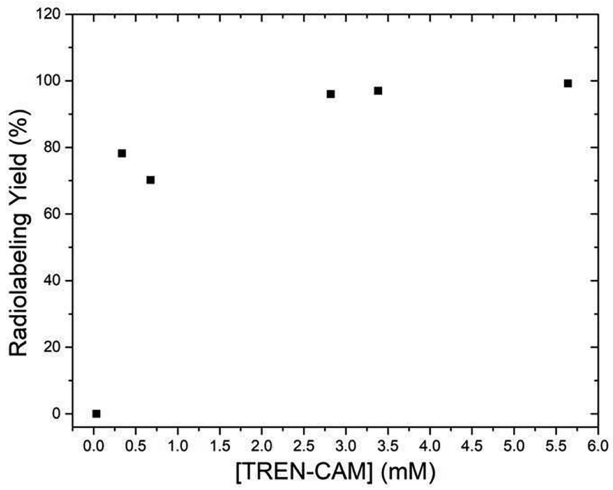

Figure 4. Effect of TREN-CAM concentration on radiolabeling yield with [^{68}Ga]$GaCl_3$.

Stability in Human Serum. The *in vitro* stability of radiolabeled ligands **1**−**4** after incubation for ≤2 h in freshly harvested human serum at 37 °C was evaluated by iTLC. The results, shown in Figure 5, indicate that although the gallium-68 complexes of TREN-CAM ([^{68}Ga]Ga-**1**) and TREN-bisGlyGlu-CAM ([^{68}Ga]Ga-**4**) were remarkably stable in human serum, almost no decomplexation was observed over

https://dx.doi.org/10.1021/acs.inorgchem.0c00975
Inorg. Chem. XXXX, XXX, XXX−XXX

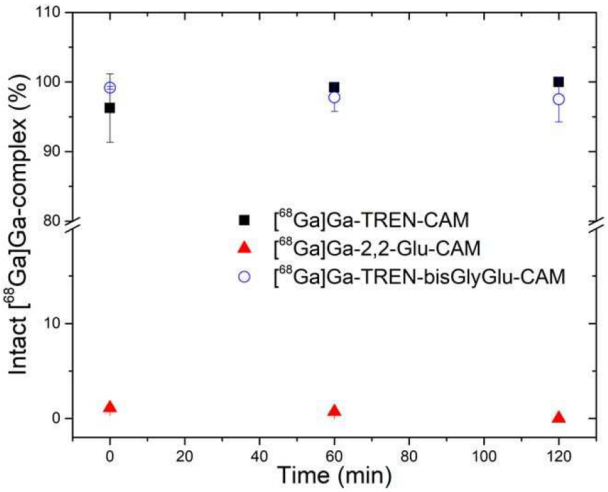

Figure 5. Stability of [^{68}Ga]Ga-TREN-CAM (**1**), [^{68}Ga]Ga-2,2-GluCAM (**2**), and [^{68}Ga]Ga-TREN-bisGlyGlu-CAM (**4**) in human serum at 37 °C. Error bars represent ±1 standard deviation (n = 3).

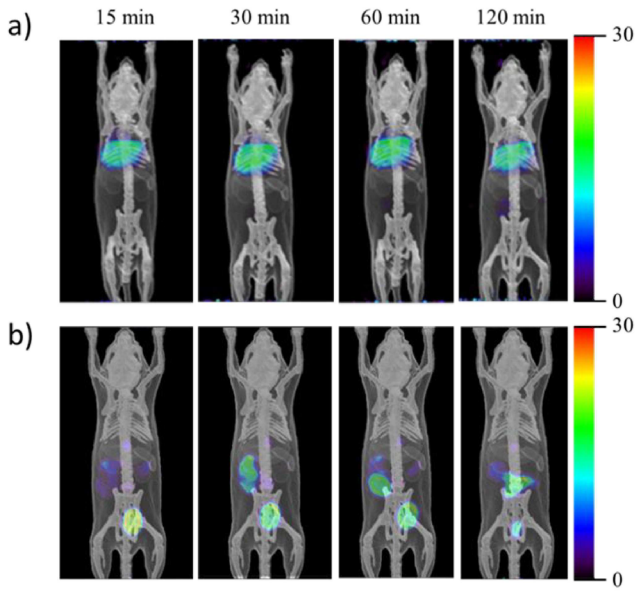

Figure 6. Representative PET images showing the distribution of (a) [^{68}Ga]$GaCl_3$ and (b) [^{68}Ga]Ga-TREN-CAM (**1**) 15, 30, 60, and 120 min postadministration with [^{68}Ga]Ga-TREN-CAM activity primarily in the bladder, gut, and kidneys. PET images were normalized to units of SUV and presented as maximum intensity projection scan (MIPS) images. The anatomic reference skeleton images are formed by using the mouse atlas registration system algorithm with information obtained from the stationary top-view planar X-ray projector and side-view optical camera. Abbreviations: GU, gut; KI, kidney; BL, bladder.

2 h (approximately twice the half-life of ^{68}Ga). However, both [^{68}Ga]Ga-2,2-Glu-CAM ([^{68}Ga]Ga-**2**) and [^{68}Ga]Ga-3,3-Glu-CAM ([^{68}Ga]Ga-**3**) decomplexed almost immediately in serum. Representative iTLC traces of the stability measurements are shown in Figure S54. Interestingly, there does not appear to be a straightforward relationship between the thermodynamic stability of the Ga^{III} complex in aqueous buffer, as determined by pGa, and the stability of the complex in serum. Indeed, Ga-2,2-GluCAM and Ga-3,3-GluCAM are both more stable than Ga-DFO; yet, both of those former complexes rapidly leach out Ga^{3+} in serum, whereas Ga-DFO does not. On the other hand, Ga-TREN-bisGlyGlu-CAM, whose stability is comparable to that of Ga-DFO, remains remarkably stable in serum. The source of this discrepancy has not been determined but could potentially be due to the faster kinetics of transmetalation with the less rigid 2,2-GluCAM and 3,3-GluCAM ligands. The TREN ligand cap of TREN-CAM and TREN-bisGlyGluCAM appears to be necessary for maintaining the stability of the gallium-68 complex in serum.

Gallium-68 PET Imaging Studies. Given its high thermodynamic stability (high pGa values), its quantitative radiochemical yield, and its excellent stability in human serum, [^{68}Ga]Ga-TREN-CAM was selected for further PET imaging studies *in vivo*. Dynamic PET/X-ray imaging studies were carried out in mice (n = 3 female) to evaluate the pharmacokinetics and biodistribution of the radiotracer. The data shown in Figure 6b strongly suggest that ^{68}Ga-radiolabeled TREN-CAM undergoes rapid renal clearance. Fifteen minutes postinjection, the radionuclide was distributed primarily to the bladder, with some gallium-68 localized in the gut and kidneys, in accordance with high urinary excretion. Importantly, the PET images show a discrete distribution of [^{68}Ga]Ga-TREN-CAM into specific soft tissues, with little to no retention in other organs such as bones. Unchelated [^{68}Ga]$GaCl_3$ has a very different biodistribution profile (Figure 6a), with accumulation in heart tissue. The vastly different biodistributions of [^{68}Ga]Ga-TREN-CAM and [^{68}Ga]$GaCl_3$ suggest that TREN-CAM does not release its gallium-68 radionuclide *in vivo*, in agreement with the high stability in serum determined above.[10,35] It is important to highlight that given the rapid clearance exhibited by [^{68}Ga]Ga-TREN-CAM, the *in vivo* biodistribution profile observed depicts mainly what can be considered as short-term high stability. This does not necessarily guarantee that (bio)macromolecular derivatives of those complexes, which would stay in circulation for longer periods of time, would remain intact *in vivo*.[3]

The *ex vivo* biodistribution of [^{68}Ga]Ga-TREN-CAM was evaluated after PET imaging on organ tissues harvested 2 h postinjection. The results, shown in Figure 7, demonstrate that the ^{68}Ga radiotracer is not exclusively cleared via renal routes. Indeed, there is a significant presence of the radiotracer in the upper gut (6.3 ± 0.8% ID/g of tissue), liver (2.0 ± 0.3% ID/g of tissue), and especially cecum feces (108.7 ± 8.9% ID/g of tissue). These results suggest that at least some [^{68}Ga]Ga-TREN-CAM also clears through the gastrointestinal tract via hepatobiliary excretion routes.[68] Importantly, though, and as needed for further targeted imaging, the *ex vivo* biodistribution study indicates that after 120 min, the radiotracer does not accumulate significantly in the organs or tissues not involved in clearance.

Biodistribution and Pharmacokinetics of Ga-TREN-CAM. Biodistribution and pharmacokinetic analysis of Ga-TREN-CAM was also carried out at higher concentrations with the nonradioactive natural isotope of gallium. This study was performed to determine if the injected dose of the metal complex and the use of a native versus a radioactive isotope affects the biodistribution and pharmacokinetic behavior of the probe. Ga^{III}-TREN-CAM was injected intravenously in the tail vein of mice (n = 3 female mice). In this case, the distribution of the Ga^{III} complex was evaluated *ex vivo* in blood and organ by inductively coupled plasma mass spectrometry (ICP-MS). As one can see from Figure 8, the biodistribution of Ga^{III}-TREN-CAM injected at large doses and monitored by

https://dx.doi.org/10.1021/acs.inorgchem.0c00975
Inorg. Chem. XXXX, XXX, XXX−XXX

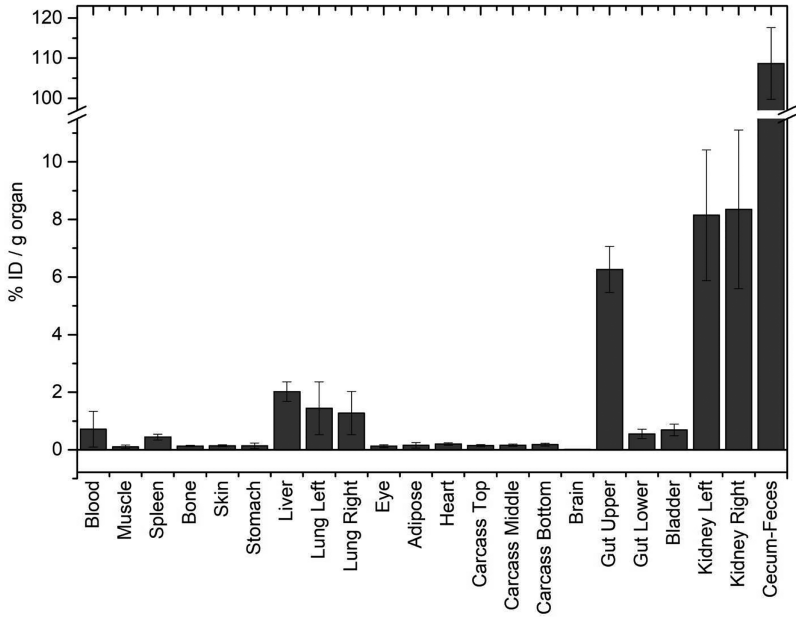

Figure 7. *Ex vivo* biodistribution pattern of [^{68}Ga]Ga-TREN-CAM 120 min postinjection. Error bars represent ±1 standard deviation (n = 3) (except for cecum feces and bladder where n = 2). % ID/g of organ is the percentage of injected dose per gram of organ weight.

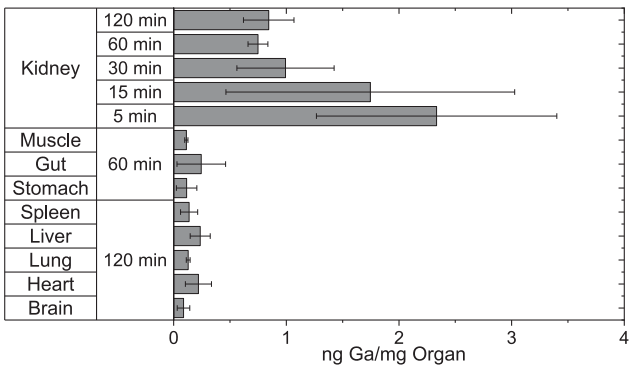

Figure 8. *Ex vivo* biodistribution of Ga-TREN-CAM in mice. Error bars represent ±1 standard deviation (n = 3).

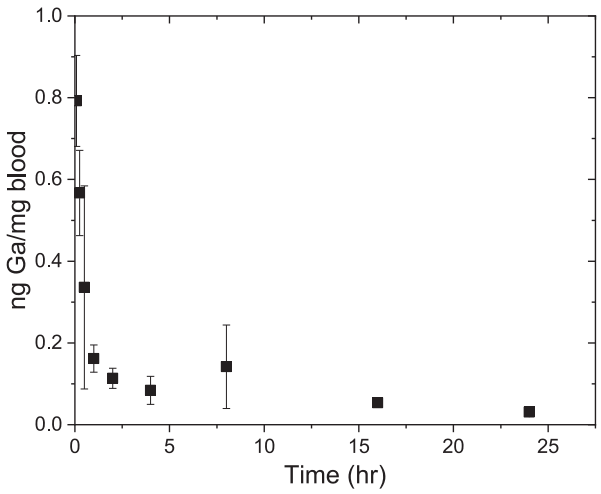

Figure 9. Blood concentration of ^{nat}Ga after injection with ^{nat}Ga-TREN-CAM in mice. Error bars represent ±1 standard deviation (n = 3).

elemental analysis follows closely that of the prior experiment by measuring the radioactivity levels of organs. In particular, the large dose of Ga observed in the kidney 2 h postinjection confirms that Ga-TREN-CAM is primarily cleared renally.

The curve of the postinjection concentration of Ga in blood versus time shown in Figure 9 is typical of the pharmacokinetics of most xenobiotic agents. Two phases are readily distinguishable, an early rapid declining phase followed by a moderately declining period. During the first phase (between time of dosing and 2 h), also known as the distribution phase, a rapid decrease in Ga concentration in plasma occurs as it is being distributed from the central compartment (circulation) into the peripheral compartments (body tissues). This phase ends when an equilibrium of Ga concentration is established between the central and peripheral compartments. The second phase is a distinctive elimination period (from 2 h onward) in which there is a more gradual decrease in plasma concentration as the ^{68}Ga chelator is excreted from the organism.

■ CONCLUSION

Tripodal tris-catecholate ligands enable rapid radiolabeling of gallium-68 in short periods of time (<10 min) at room temperature and non-acidic pH. These rapid kinetics, which are attributed to the acyclic nature of the ligands, give them a distinct advantage over macrocyclic ligands such as DOTA that require high temperatures, acidic conditions, and long reaction times to achieve sufficient radiolabeling. Addition of a peripheral carboxylate group for further conjugation to a targeting moiety can be achieved via modification of the ligand cap and incorporation of a glutamic acid residue. It is noteworthy that the modular nature of the synthesis enables facile incorporation of amine or thiol peripheral groups in lieu of the carboxylate one if so desired for further bioconjugation. Unfortunately, addition of the amino acid in the ligand backbone affects the tight hydrogen-bonding network of the ligand cap. As a result, even though 2,2-Glu-CAM, 3,3-Glu-CAM, and TREN-bisGlyGlu-CAM still bind Ga^{III} rapidly at room temperature, their corresponding Ga^{III} complex is less stable than Ga-TREN-CAM. Nonetheless, these complexes

https://dx.doi.org/10.1021/acs.inorgchem.0c00975
Inorg. Chem. XXXX, XXX, XXX−XXX

remain at least as stable as those of common acyclic gallium chelators evaluated for PET, such as Ga-DFO. Interestingly, trends of stability in buffer do not correspond to those observed in human serum. Of the four gallium-68 complexes evaluated, two, [^{68}Ga]Ga-TREN-CAM and [^{68}Ga]Ga-TREN-bisGlyGluCAM, were highly stable in human serum, with nearly no dechelation observed over 2 h. Importantly, PET imaging analysis in healthy mice showed that Ga-TREN-CAM displays high stability *in vivo*, in agreement with the relative conditional stability observed *in vitro*. *In vivo* PET studies in mice and *ex vivo* biodistribution analyses of [^{68}Ga]Ga-TREN-CAM suggest that, after tail vein injection, the radiotracer is cleared rapidly from mice (<15 min) primarily via renal routes. The high stability of Ga-TREN-bisGlyGlu-CAM in serum for extended periods of time combined with the high radiolabeling yields obtained after short reaction times at room temperature and the presence of a functional group for further bioconjugation to targeting group renders TREN-bisGlyGlu-CAM a promising target for gallium radiopharmaceuticals.

■ EXPERIMENTAL SECTION

General Considerations. Unless otherwise stated, all reagents were purchased from commercial sources and used without further purification. Flash chromatography was performed on silica gel SiliFlash F60 40−63 μm. Distilled water was further purified by a Millipore Simplicity UV system (resistivity of 18 × 10^6 Ω). Deuterated solvents were obtained from Cambridge Isotope Laboratories (Tewskbury, MA). ^{1}H and ^{13}C NMR spectra were recorded at room temperature on a Bruker Advance III 400 spectrometer at 400 and 100 MHz, respectively, at the LeClaire-Dow Characterization Facility of the Department of Chemistry at the University of Minnesota. Residual solvent peaks were used as the internal reference. ^{1}H NMR data are reported as follows: chemical shifts (δ, ppm), multiplicity (s, singlet; d, doublet; t, triplet; m, multiplet; br, broad), coupling constants (Hz), and integration. ^{13}C NMR data are reported as chemical shifts (δ, ppm). Mass spectra were recorded on a Bruker BioTOF II ESI/TOF-MS instrument at the Waters Center for Innovation in Mass Spectrometry of the Department of Chemistry at the University of Minnesota. Ultraviolet−visible spectra were recorded on a Varian Cary 100 Bio Spectrometer with 1 cm quartz cuvettes in TRIS(aq) buffer (0.01 M) and KCl (0.1 M) (pH 7.4). Semipreparative high-performance liquid chromatography (HPLC) was performed with a Varian Prostar 210 HPLC instrument (Agilent, Santa Clara, CA) equipped with a Varian ProStar 335 diode array detector and an Agilent Zorbax Eclipse XDB-C18 column (5 μm pore size, 9.4 mm × 250 mm). Unless specified otherwise, HPLC measurements were performed at a flow rate of 1.0 mL min^{-1} with the following elution condition: 15% CH_3CN/85% water from 0 to 2 min, followed by a linear gradient to 100% CH_3CN from 2 to 23 min, and 15% CH_3CN/85% water from 30 to 32 min. All pH measurements were performed using a Thermo Scientific Ag/AgCl refillable probe and a Thermo Orion 3 Benchtop pH meter.

Synthesis and Characterization. CAM(Bn) (**5**),[51] CAM(Bn)-thiaz (**7**),[54] Glu(^{t}Bu)CAM(Bn) (**10**),[55] and GlyCAM(Bn) (**14**)[55] were prepared according to literature procedures with successful synthesis established by LR MS and ^{1}H NMR spectroscopy.

TREN-CAM(Bn) (6). To an ice-cooled solution of CAM(Bn) acid (**5**, 1.04 g, 3.10 mmol) and tris(2-aminoethyl)amine (TREN, 151 mg, 1.03 mmol) in anhydrous dichloromethane (30 mL) under N_2(g) was added diisopropylethylamine (DIPEA, 632 μL, 3.63 mmol) followed by TBTU (1.09 g, 3.40 mmol). The resulting mixture was stirred at room temperature for 24 h. The reaction mixture was concentrated under reduced pressure. The resulting oil was resuspended in ethyl acetate (100 mL) and washed successively with saturated $NaHCO_3$(aq) (5 × 50 mL) and saturated NaCl(aq) (2 × 50 mL). The organic layer was dried over Na_2SO_4(s), filtered, and concentrated under reduced pressure. The crude product was purified by flash chromatography over silica eluting with 5% CH_3OH/95% CH_2Cl_2 to yield TREN-CAM(Bn) (**6**) as a light-yellow oil (0.57 g, 50%). ^{1}H NMR (400 MHz, $CDCl_3$): δ 7.80 (t, J = 6 Hz, 3H), 7.62−7.61 (m, 3H), 7.42−7.40 (m, 6H), 7.37−7.32 (m, 9H), 7.27−7.21 (m, 15H), 7.07−7.06 (m, 6H), 5.07 (s, 6H), 5.02 (s, 6H), 3.15 (q, J = 6 Hz, 6H), 2.32 (t, J = 7 Hz, 6H). ^{13}C NMR (100 MHz, $CDCl_3$): δ 165.2, 151.7, 146.7, 136.6, 136.5, 128.6 (×3), 128.2, 127.8, 127.6, 124.3, 123.1, 116.8, 76.2, 71.2, 52.5, 37.3. ESI-HR-MS. Calcd for $C_{69}H_{67}N_4O_9$ [M + H]$^+$: m/z 1095.4908. Found: m/z 1095.4971.

TREN-CAM (1). TREN-CAM(Bn) (**6**, 54 mg, 49 μmol) was dissolved in a mixture of glacial acetic acid and 12 N HCl [1:1 (v/v), 2 mL] and stirred at room temperature under N_2(g) for 24 h. The volatiles were then removed under reduced pressure to yield the HCl salt of the free ligand TREN-CAM as an off-white solid. (**1**, 32 mg, quant. yield). ^{1}H NMR (400 MHz, CD_3OD): δ 7.13 (dd, J = 8 Hz, J = 2 Hz, 3H), 6.90 (dd, J = 8 Hz, J = 2 Hz, 3H), 6.63 (t, J = 8 Hz, 3H), 3.85 (t, J = 6 Hz, 6H), 3.67 (t, J = 6 Hz, 6H). ^{13}C NMR (100 MHz, CD_3OD): δ 172.7, 149.7, 147.1, 120.0, 119.9, 119.6, 116.4, 55.4, 36.0. ESI-HR-MS. Calcd for $C_{27}H_{31}N_4O_9$ [M + H]$^+$: m/z 555.2091. Found: m/z 555.2062.

Ga-TREN-CAM (Ga-1). The deprotected ligand **1** (125 mg, 225 μmol) and KOH (37.8 mg, 674 μmol) were first mixed in methanol (4 mL). Next, Ga(acac)$_3$ (82.5 mg, 225 μmol) was added, and the resulting crude stirred overnight at room temperature. The product was precipitated with diethyl ether (10 mL), separated off, and dried under reduced pressure to yield Ga-TREN-CAM as a beige powder (**Ga-1**, 158 mg, 95%). ^{1}H NMR (400 MHz, DMSO-d_6): δ 11.12 (s, 3H), 6.78 (d, J = 8.1 Hz, 3H), 6.44 (d, J = 7.2 Hz, 3H), 6.10 (t, J = 7.7 Hz, 3H), 3.37 (s, 6H), 2.33 (s, 6H). ^{13}C NMR (100 MHz, DMSO-d_6): δ 168.2, 158.7, 155.9, 114.6, 114.1, 112.0, 111.7, 54.8, 34.3. ESI-HR-MS. Calcd for $C_{27}H_{26}GaN_4O_9$ [M + 2H]$^-$: m/z 619.0956. Found: m/z 619.0972.

2,2-CAM(Bn) (8). CAM(Bn)thiaz (**7**, 1.32 g, 3.02 mmol) and diethylenetriamine (122 μL, 1.13 mmol) were dissolved in anhydrous dichloromethane (75 mL). The resulting mixture was stirred at room temperature under N_2(g) for 48 h. The reaction mixture was then concentrated under reduced pressure. The crude product was purified by flash chromatography over silica eluting with 5% CH_3OH/95% CH_2Cl_2 to yield intermediate 2,2-CAM(Bn) (**8**, 0.48 g, 58%) as a colorless oil. ^{1}H NMR (400 MHz, $CDCl_3$): δ 8.05 (t, J = 6 Hz, 2H), 7.66 (t, J = 4 Hz, 2H), 7.40−7.39 (m, 4H), 7.35−7.25 (m, 16H), 7.06 (d, J = 5 Hz, 4H), 5.06 (s, 4H), 5.03 (s, 4H), 3.26 (q, J = 6 Hz, 4H), 2.50 (t, J = 6 Hz, 4H). ^{13}C NMR (100 MHz, $CDCl_3$): δ 165.5, 151.8, 146.8, 136.6, 136.5, 128.7 (×2), 128.6 (×2), 128.2, 127.7, 127.6, 124.4, 123.1, 116.9, 76.3, 71.2, 53.6, 48.1, 39.3. ESI-LR-MS. Calcd for $C_{46}H_{46}N_3O_6$ [M + H]$^+$: m/z 736.34. Found: m/z 736.44.

2,2-Glu(^{t}Bu)-CAM(Bn) (11). DIPEA (198 μL, 0.114 mmol) followed by TBTU (0.28 g, 0.87 mmol) were added to an ice-cooled solution of 2,2-CAM(Bn) (**8**, 0.49 g 0.67 mmol) and Glu(^{t}Bu)CAM-(Bn) (**10**, 0.43 g, 0.84 mmol) in anhydrous dichloromethane (15 mL) under N_2(g). The resulting mixture was stirred at room temperature for 24 h and then concentrated under reduced pressure. The resulting oil was then suspended in ethyl acetate (100 mL) and washed successively with saturated $NaHCO_3$(aq) (5 × 50 mL) and saturated NaCl(aq) (2 × 50 mL). The organic layer was dried over Na_2SO_4(s), filtered, and concentrated under reduced pressure. The crude product was purified by flash chromatography over silica, eluting with 40% ethyl acetate/60% hexanes to yield 2,2-Glu(^{t}Bu)-CAM(Bn) as a colorless oil (**11**, 0.58 g, 71%). ^{1}H NMR (400 MHz, $CDCl_3$): δ 8.57 (d, J = 8 Hz, 1H), 8.13 (s, 1H), 8.02 (t, J = 6 Hz, 1H), 7.65−7.57 (m, 3H), 7.45−7.17 (m, 31H), 7.07−7.01 (m, 6H), 5.18−4.98 (m, 13H), 3.66−3.21 (m, 8H), 2.24−2.08 (m, 2H), 1.95−1.90 (m, 1H), 1.62−1.52 (m, 1H), 1.37 (s, 9H). ^{13}C NMR (100 MHz, $CDCl_3$): δ 172.6, 172.0, 166.0, 165.7, 164.9, 151.9, 151.8, 151.7, 147.0, 146.8 (×2), 136.6 (×3), 136.4 (×2), 129.3, 129.0, 128.8, 128.7 (×2), 128.6, 128.4 (×2), 128.3 (×2), 128.0, 127.9, 127.8, 127.7 (×2), 127.0, 124.3 (×2), 124.2, 123.3, 123.1 (×2), 117.2, 117.1, 117.0, 80.4, 76.4, 76.2, 76.1, 71.4, 71.2 (×2), 49.0, 47.0, 45.8, 38.5, 37.8, 31.2, 28.2, 28.0. ESI-LR-MS. Calcd for $C_{76}H_{77}N_4O_{12}$ [M + H]$^+$: m/z 1237.55. Found: m/z 1237.57.

https://dx.doi.org/10.1021/acs.inorgchem.0c00975
Inorg. Chem. XXXX, XXX, XXX−XXX

2,2-Glu-CAM (2). 2,2-Glu(^{t}Bu)-CAM(Bn) (**11**, 240 mg, 194 μmol) was dissolved in a mixture of glacial acetic acid and 12 N HCl [1:1 (v/v), 12 mL] and stirred at room temperature under N_2(g) for 30 h. The volatiles were removed under reduced pressure to yield the free ligand (**2**) as an off-white solid (98.0 mg, 80%). ^{1}H NMR (400 MHz, DMF-d_7): δ 9.15 (s, 1H), 8.93 (s, 1H), 7.50−7.24 (m, 4H), 7.02−6.95 (m, 3H), 6.76−6.67 (m, 3H), 4.62 (dd, J_1 = 9 Hz, J_2 = 6 Hz, 1H), 3.66 (br s, 4H), 3.16 (br s, 4H), 2.52 (t, J = 8 Hz, 2H), 2.31−2.25 (m, 1H), 2.19−2.15 (m, 1H). ^{13}C NMR (100 MHz, CD_3OD): δ 173.6, 173.4, 172.8, 171.2, 150.2, 149.9, 147.3, 147.2, 120.0, 119.9 (×2), 119.8, 119.3, 119.1, 116.6, 116.3, 53.2, 49.6, 37.4, 31.1, 27.4. ESI-HR-MS. Calcd for $C_{30}H_{31}N_4O_{12}$ [M − H]$^-$: m/z 639.1938. Found: m/z 639.1963.

Ga-2,2-Glu-CAM (Ga-2). 2,2-Glu-CAM (**2**, 114 mg, 0.179 mmol) and KOH (30 mg, 0.53 mmol) were mixed in methanol (5 mL). Once everything was dissolved, Ga(acac$_3$) (65.4 mg, 0.178 mmol) was added. The resulting mixture was stirred at room temperature overnight. After this time, the compound was precipitated off by addition of diethyl ether (9 mL), separated off, and dried under reduced pressure to yield Ga-2,2-Glu-CAM as an off-white solid (**Ga-2**, 116.4 mg, 80%). ^{1}H NMR (400 MHz, DMSO-d_6): δ 10.56 (s, 1H), 7.31−7.13 (m, 1H), 6.92 (d, J = 8.1 Hz, 1H), 6.49 (d, J = 7.4 Hz, 1H), 6.26 (t, J = 7.7 Hz, 1H), 4.34 (s, 1H), ∼3.44 (4H) signal overlapped by a water peak, 2.71 (s, 4H), 2.36−2.19 (m, 2H), 2.00−1.89 (m, 2H). ESI-LR-MS. Calcd for $C_{30}H_{28}GaN_4O_{12}$ [M + 2H]$^-$: m/z 705.10. Found: m/z 705.20.

3,3-CAM(Bn) (9). The bis-amide 3,3-CAM(Bn) (**9**) was prepared according to the literature procedure reported by Allred et al.[54] and purified by flash chromatography over silica eluting with 10% CH_3OH/90% CH_2Cl_2 to yield **9** as a white powder (0.49 g, 82%). ^{1}H NMR (400 MHz, $CDCl_3$): δ 8.10 (m, 2H), 7.63 (dd, J_1 = 7 Hz, J_2 = 3 Hz, 2H), 7.43−7.41 (m, 4H), 7.36−7.29 (m, 16H), 7.08−7.06 (m, 4H), 5.08 (s, 4H), 5.05 (s, 4H), 4.74 (br s, 1H), 3.32−3.30 (m, 4H), 2.50−2.46 (m, 4H), 1.63−1.60 (m, 4H). ^{13}C NMR (100 MHz, $CDCl_3$): δ 165.8, 151.7, 146.7, 136.5, 136.4, 128.8, 128.7 (×2), 128.3, 127.7, 127.5, 124.4, 123.0, 117.0, 76.4, 71.2, 50.2, 46.6, 37.2, 28.5. Calcd for $C_{48}H_{50}N_3O_6$ [M + H]$^+$: m/z 764.37. Found: m/z 764.38.

3,3-Glu(^{t}Bu)-CAM(Bn) (12). DIPEA (192 μL, 1.10 mmol) followed by TBTU (0.271 g, 844 μmol) were added to a solution of 3,3-CAM(Bn) (**9**, 0.49 g, 0.65 mmol) and Glu(^{t}Bu)CAM(Bn) (**10**, 0.46 g, 0.88 mmol) in anhydrous dichloromethane (16 mL) cooled to 0 °C under N_2(g). The resulting mixture was stirred at room temperature for 24 h. The reaction mixture was concentrated under reduced pressure. The resulting oil was then resuspended in ethyl acetate (100 mL) and washed successively with saturated $NaHCO_3$(aq) (5 × 50 mL) and saturated NaCl(aq) (2 × 50 mL). The organic layer was dried over Na_2SO_4(s), filtered, and concentrated under reduced pressure. The crude product was purified by flash chromatography over silica, eluting with a gradient of 100% hexanes to 100% ethyl acetate to yield the protected ligand 3,3-Glu(^{t}Bu)-CAM(Bn) as a colorless oil (**12**, 0.55 g, 67%). ^{1}H NMR (400 MHz, $CDCl_3$): δ 8.54 (d, J = 8 Hz, 1H), 8.04−8.00 (m, 2H), 7.69−7.61 (m, 3H), 7.41−7.28 (m, 24H), 7.22−7.16 (m, 6H), 7.08−7.02 (m, 6H), 5.19 (m, 1H), 5.09−4.99 (m, 12H), 3.47−2.98 (m, 8H), 2.27−2.10 (m, 2H), 1.97−1.89 (m, 1H), 1.77−1.68 (m, 2H), 1.61−1.50 (m, 3H), 1.40 (s, 9H). ^{13}C NMR (100 MHz, $CDCl_3$): δ 172.0, 171.8, 165.6, 165.4, 165.0, 151.9, 151.8 (×2), 147.0, 146.8, 146.7, 136.7, 136.6 (×3), 136.4, 136.3, 129.2, 128.9, 128.8 (×2), 128.7 (×4), 128.6, 128.5, 128.4, 128.3 (×2), 128.2, 127.9 (×2), 127.7, 127.6, 127.1, 124.4, 124.3, 124.2 (×2), 123.0 (×2), 117.3, 117.0, 116.8, 80.5, 76.4, 76.2, 76.1, 71.3 (×2), 71.2, 53.7, 48.7, 45.3, 43.5, 37.2, 36.9, 31.1, 29.1, 28.4, 28.2, 27.7. ESI-LR-MS. Calcd for $C_{78}H_{80}N_4NaO_{12}$ [M + Na]$^+$: m/z 1287.57. Found: m/z 1287.58.

3,3-Glu-CAM (3). 3,3-Glu(^{t}Bu)-CAM(Bn) (**12**, 0.10 g, 81 μmol) was dissolved in glacial acetic acid and 12 M HCl [1:1 (v/v), 3 mL] and stirred at room temperature under N_2(g) for 30 h. The volatiles were then removed under reduced pressure to yield 3,3-Glu-CAM as an off-white solid (**3**, 58 mg, quant. yield). ^{1}H NMR (400 MHz, CD_3OD): δ 7.32−7.22 (m, 4H), 6.95−6.93 (m, 3H), 6.75−6.69 (m, 3H), 4.68 (dd, J_1 = 9 Hz, J_2 = 5 Hz, 1H), 3.51 (t, J = 7 Hz, 4H), 3.08 (t, J = 7 Hz, 4H), 2.46 (t, J = 7 Hz, 2H), 2.30−2.28 (m, 1H), 2.11−2.00 (m, 5H). ^{13}C NMR (100 MHz, CD_3OD): δ 173.6, 173.4, 172.1, 171.2, 150.1, 149.9, 147.3, 147.2, 119.9, 119.8 (×2), 119.7, 119.3, 118.9, 116.6, 116.5, 53.2, 46.7, 37.1, 31.1, 27.6, 27.4. ESI-HR-MS. Calcd for $C_{32}H_{35}N_4O_{12}$ [M − H]$^-$: m/z 667.2251. Found: m/z 667.2248.

Ga-3,3-Glu-CAM (Ga-3). The deprotected ligand Ga-3,3-Glu-CAM (**3**, 59.4 mg, 88.8 μmol) was first dissolved in methanol (3 mL), followed by the addition of KOH (15.0 mg, 267 μmol). Next, Ga(acac)$_3$ (32.6 mg, 88.8 μmol) was added, and the resulting mixture stirred at room temperature for 18 h. The desired product was precipitated off by addition of diethyl ether (9 mL). The white solid was then separated off and dried under reduced pressure (**Ga-3**, 58.2 mg, 78%). ^{1}H NMR (400 MHz, DMF-d_7): δ 10.28−10.55 (m, 2H), 7.28−6.99 (m, 4H), 6.79−6.63 (m, 3H), 6.25−6.29 (m, 3H), 4.60−4.70 (m, 1H), 3.78−3.78 (m, 8H + ether), 2.44 (br, 2H), 2.16−1.98 (m, 6H + acetic acid/acetate). ESI-HR-MS. Calcd for $C_{32}H_{32}GaN_4O_{12}$ [M + 2H]$^-$: m/z 733.1274. Found: m/z 733.1224.

TREN-Glu(^{t}Bu)-CAM(Bn) (13). *N*-Hydroxysuccinimide (98 mg, 0.85 mmol) was added to a stirred solution of Glu(^{t}Bu)CAM(Bn) (**10**, 0.37 g, 0.71 mmol) in anhydrous 1,4-dioxane (10 mL), and the resulting reaction mixture was cooled to 0 °C. *N*-Ethyl-*N*′-(3-dimethylaminopropyl)carbodiimide hydrochloride (EDC·HCl, 163 mg, 850 μmol) was added to the reaction mixture that was then further stirred at room temperature for 24 h. The resulting active ester was further added to a prestirred solution of tris(2-aminoethyl)amine (TREN, 603 mg, 4.13 mmol) and DIPEA (2.3 mL, 13 mmol) in anhydrous 1,4-dioxane (5 mL). The reaction mixture was stirred at room temperature for 30 h and then concentrated under reduced pressure. The crude product was dissolved in dichloromethane (50 mL) and washed with water (2 × 20 mL). The organic layer was dried with $MgSO_4$(s). The volatiles were then removed under reduced pressure to yield TREN-Glu(^{t}Bu)-CAM(Bn) (**13**) as a yellow paste (0.42 g, 91%) that was used immediately in the next step without further purification. ^{1}H NMR (400 MHz, $CDCl_3$): δ 8.46 (d, J = 8 Hz, 1H), 8.07 (br, 1H), 7.57 (dd, J_1 = 7 Hz, J_2 = 3 Hz, 1H), 7.43−7.26 (m, 7H), 7.24−7.16 (m, 3H), 7.11−6.97 (m, 2H), 5.17−4.91 (m, 4H), 4.77−4.39 (m, 1H), 2.75−2.38 (m, 12H), 2.20−2.09 (m, 2H), 2.03−1.90 (m, 1H), 1.72−1.51 (m, 1H), 1.33 (m, 9H). ESI-LR-MS. Calcd for $C_{36}H_{48}N_5O_6$ [M − H]$^-$: m/z 646.36. Found: m/z 646.29.

TREN-bisGlyGlu(^{t}Bu)-CAM(Bn) (15). To a stirred solution of GlyCAM(Bn) (**14**, 0.27 g, 0.69 mmol) in anhydrous dichloromethane (10 mL) was added *N*-hydroxysuccinimide (NHS, 0.106 g, 0.921 mmol), and the resulting reaction mixture was cooled to 0 °C. EDC (0.173 g, 0.902 mmol) was added, and the reaction mixture was stirred at room temperature for 24 h. The resulting active ester was then added to a prestirred solution of TREN-Glu(^{t}Bu)-CAM(Bn) (**13**, 0.15 g, 0.23 mmol) and DIPEA (620 μL, 3.47 mmol) in dichloromethane (5 mL). The reaction mixture was stirred at room temperature for 30 h and then concentrated under reduced pressure. The crude product was dissolved in dichloromethane (60 mL) and washed with water (2 × 30 mL). The organic layer was dried with $MgSO_4$(s), and the solvent removed under reduced pressure. The crude product was purified by flash chromatography over silica eluting with 5% CH_3OH/95% CH_2Cl_2 to yield TREN-bisGlyGlu(^{t}Bu)-CAM(Bn) as a yellow oil (**13**, 0.32 g, 40%). ^{1}H NMR (400 MHz, $CDCl_3$): δ 8.64−8.56 (m, 3H), 7.75−7.60 (m, 6H), 7.48−7.31 (m, 30H), 7.10 (b, 6H), 5.19−5.09 (m, 12H), 4.59−4.52 (m, 1H), 4.02−3.88 (m, 4H), 3.50−3.01 (m, 6H), 2.67−2.47 (m, 6H), 2.25−2.18 (m, 2H), 2.03−1.98 (m, 1H), 1.77−1.72 (m, 1H), 1.41 (s, 9H). ^{13}C NMR (100 MHz, $CDCl_3$): δ 172.0, 171.9, 171.8, 171.7, 169.6, 169.5, 166.0, 165.5, 151.9, 151.8, 147.0 (×2), 136.4, 136.3 (×2), 136.2 136.1, 129.4, 129.3 (×2), 129.2, 128.7 (×2), 128.6 (×2), 128.5, 128.3, 128.2, 128.0, 127.9, 127.8, 127.7, 127.0, 126.5, 124.4, 123.1, 122.9, 117.3, 80.3, 76.3, 76.2, 71.3 (×2), 54.4, 54.0, 53.5, 43.8, 38.6, 38.3, 31.9, 28.1, 27.3. ESI-LR-MS. Calcd for $C_{82}H_{88}N_7O_{14}$ [M + H]$^+$: m/z 1394.64. Found: m/z 1394.67.

TREN-bisGlyGlu-CAM (4). TREN-bisGlyGlu(^{t}Bu)-CAM(Bn) (**15**, 29 mg, 21 μmol) was dissolved in glacial acetic acid and 12 M

https://dx.doi.org/10.1021/acs.inorgchem.0c00975
Inorg. Chem. XXXX, XXX, XXX−XXX

HCl [1:1 (v/v), 2 mL] and stirred at room temperature under N_2(g) for 20 h. The volatiles were removed under reduced pressure to yield the HCl salt of the free ligand TREN-bisGlyGlu-CAM as an off-white solid. (**4**, 17 mg, 96%). ^{1}H NMR (400 MHz, CD_3OD): δ 7.32−7.25 (m, 3H), 6.93 (d, J = 8 Hz, 3H), 6.74−6.69 (m, 3H), 4.58−4.54 (m, 1H), 4.04 (br, s, 4H), 3.61−3.46 (m, 12H), 2.47−2.43 (m, 2H), 2.24−2.21 (m, 1H), 2.09−2.02 (m, 1H). ^{13}C NMR (100 MHz, CD_3OD): δ 173.5, 171.8, 149.8, 147.0, 129.6, 129.5, 129.4, 120.0, 119.9, 119.7, 119.5, 116.7, 116.5, 55.6, 54.8, 43.9, 36.1, 36.0, 31.3, 27.5, 20.8. ESI-HR-MS. Calcd for $C_{36}H_{42}N_7O_{14}$ [M − H]$^-$: m/z 796.2790. Found: m/z 796.2858.

Ga-TREN-bisGlyGlu-CAM (Ga-4). TREN-bisGlyGlu-CAM (**4**, 59.8 mg, 75.0 μmol) and KOH (12.6 mg, 225 μmol) were first dissolved in methanol (2 mL), followed by the addition of Ga(acac)$_3$ (27.8 mg, 75.7 μmol). The resulting product was precipitated out of solution by addition of diethyl ether. The solid was separated off and dried under reduced pressure to yield Ga-TREN-bisGlyGlu-CAM as a white powder (**Ga-4**, 33.3 mg, 54%). For ^{1}H NMR (400 MHz, DMSO-d_6), the existence of multiple isomers in solution as well as the reduced solubility of this coordination compound that seems to facilitate the formation of aggregates results in a complex NMR spectrum. Assignment of signals is challenging, and thus, the ^{1}H NMR spectrum is instead shown in the Supporting Information. ESI-HRMS. Calcd for $C_{36}H_{39}GaN_7O_{14}$ [M + 2H]$^-$: m/z 862.1811. Found: m/z 862.1763.

Solution Thermodynamics: Competition Titrations. Samples containing known concentrations of ligand, $GaCl_3$ (0.01−1 equiv), and DFO mesylate salt (0.01−100 equiv) were prepared in Tris buffer (10 mM, pH 7.4) with KCl (0.1 M). The pH of all solutions was adjusted to 7.40 with HCl(aq) or KOH(aq) as necessary and diluted to identical volumes. All samples were equilibrated at 25 °C for 24 h, after which UV−vis spectra were recorded. The concentrations of the free and complexed ligand in each solution were averaged over 10 wavelengths by using solutions of L and GaL at the same concentration and under the conditions as the references. Using the known pGa value for DFO (21.2),[35] the concentration of the competing ligand necessary to generate an equal partition of Ga^{3+} between the ligand of interest and the competitor occurs at the x-intercept of the log−log plot (Figure 3), which gives the difference in pGa values between DFO and the ligand of interest (Table 1).

Method of Cyclotron Production and Purification of [^{68}Ga]GaCl$_3$. The ^{68}Ga isotope was produced with a GE PETtrace (16.3 MeV energy) cyclotron using a liquid target via the ^{68}Zn-(p,n)^{68}Ga nuclear reaction as described previously.[66] In brief, a 1 M solution of isotopically enriched (>99%) [^{68}Zn]Zn(NO$_3$)$_2$ in 1.1 N HNO$_3$(aq) was irradiated with a proton beam at 40 μA for 60 min. After irradiation, the solution was transferred to a hot cell equipped with an automated radiochemistry synthesis module (Trasis All-in-One), purified with a hydroxamate resin cartridge (100 mg), and concentrated on an anion exchange resin (Ag-1X-8, 400 mg) as described previously.[67,69] The final [^{68}Ga]GaCl$_3$ was eluted with 1.0 mL of water from anion exchange resin.[67] The purified [^{68}Ga]GaCl$_3$ solution was manually transferred to another hot cell to perform manual radiolabeling of different enterobactin-based analogues.

Radiolabeling of Enterobactin Analogues with [^{68}Ga]GaCl$_3$. Radiolabeling of each ligand was performed between pH 8.5 and 9.0 at room temperature (25 °C). In brief, the ligands (600 μg) were separately suspended in 1.5 mL of water and the pH of the resulting mixture were adjusted to ∼7.5−8.0 using 1 M NaOH(aq) until the solution became clear. Separately, the solution of [^{68}Ga]GaCl$_3$ was adjusted to 8.0−9.0 with 1 M NaOH. One milliliter of the pH-adjusted solution of cyclotron-produced [^{68}Ga]GaCl$_3$ was subsequently added to the solution of the ligand, and the reaction mixture was stirred at room temperature for 10 min. Reaction progress was measured by instant thin-layer chromatography (i-TLC) using a 1:1 mixture of methanol and 1 M ammonium acetate as the mobile phase (for ^{68}Ga complexes, f > 0.9; free [^{68}Ga]Ga^{3+} R_f = 0). The radiochemical purity was assessed using a rad-TLC scanner (BioScan, Eckert Ziegler, Berlin, Germany). The percentage of intact radiolabeled complex was calculated as follows: radiochemical purity = 100[(radioactivity at solvent front)/(radioactivity at origin + radioactivity at solvent front)]. If the radiochemical purities of the ^{68}Ga-enterobactin-based analogues (**2**−**4**) were found to be <95%, the complexes were purified by passing the solution through a CM Sep-Pak Light cartridge, thereby stripping the free [^{68}Ga]Ga^{3+} ions from the solution. The CM Sep-Pak cartridge was preactivated with 2 mL of water followed by 10 mL of air before use.

Dilute hydrochloric acid and sterile water were added to formulate ^{68}Ga-labeled TREN-CAM analogue solutions to contain approximately 0.9% NaCl at pH ∼7.2. Final solutions were filtered through a 0.2 μM sterile filter and rechecked for radiochemical purity using iTLC before use.

Evaluation of *In Vitro* Serum Stability. The stabilities of radiolabeled ligands were determined by measuring the radiochemical purity of each complex after incubation in human serum at 37 °C for 0 and 2 h. In each case, the pH was maintained between 8 and 8.5. At each incubation interval, the relative amount of radioactivity associated with free [^{68}Ga]Ga^{3+} (origin) and radiolabeled complex (solvent front) was determined using iTLC as described above.

Gallium-68 PET Imaging and Biodistribution Studies. To determine the biodistribution and pharmacokinetics of the imaging agent, three female BalbC mice (Envigo, Indianapolis, IN) were injected with [^{68}Ga]Ga-TREN-CAM [**1**, 8.8−33.3 μg total of injected labeled (0.3−1.2 MBq) and unlabeled TREN-CAM per animal] via tail vein injection. At 15, 30, 60, and 120 min postinjection, anesthetized animals underwent 10 min PET scans using a small animal PET/X-ray system (Sofie BioSystems Genesys4, Culver City, CA). The anatomic reference skeleton images were formed by using the mouse atlas registration system algorithm with information obtained from the stationary top-view planar X-ray projector and side-view optical camera. PET images were normalized to units of standardized uptake value {SUV = (activity concentration in tissue)/[(injected dose)/(g of whole body weight)]} and presented as maximum intensity projection scan (MIPS) images. To determine the biodistribution of [^{68}Ga]Ga-TREN-CAM (**1**), the mice were sacrificed after the final imaging time point (120 min) and organ tissues were harvested. The radioactivity in organ tissues was counted using a gamma counter; the measurements were decay-corrected to the time of [^{68}Ga]Ga-TREN-CAM injection, and the SUV was calculated.

Biodistribution Experiments. Thirty female mice (CD-1, 6−8 weeks of age, Envigo) were injected intravenously with Ga-TREN-CAM (1 mg/kg in PBS), and groups of three animals were euthanized at specific time points (5 min, 15 min, 30 min, 1 h, 2 h, 4 h, 8 h, 16 h, and 24 h) over a 24 h period. The blood, brain, heart, lung, liver, spleen, stomach, cecum, muscle (diaphragm), and kidney were collected from each animal and stored at −20 °C. Tissues were boiled in HNO$_3$ (∼10%) until no cloudiness remained in the sample (∼8 h). Samples were diluted with mQ water to equivalent volumes and analyzed for Ga by ICP-MS (ALS Environmental, Salt Lake City, UT). Data obtained from blood were subjected to pharmacokinetic analysis (WinNonlin software, Certara USA, Inc., Princeton, NJ) using a noncompartmental model.

■ ASSOCIATED CONTENT

Supporting Information

The Supporting Information is available free of charge at https://pubs.acs.org/doi/10.1021/acs.inorgchem.0c00975.

Characterization data, including ^{1}H and ^{13}C NMR data of intermediates and final ligands, ESI-MS data of the intermediates and ligands, HPLC chromatograms of the ligands, and UV−visible spectra of the ligands and respective Ga^{III} complexes (PDF)

https://dx.doi.org/10.1021/acs.inorgchem.0c00975
Inorg. Chem. XXXX, XXX, XXX−XXX

AUTHOR INFORMATION

Corresponding Authors

Valérie C. Pierre − *Department of Chemistry, University of Minnesota, Minneapolis, Minnesota 55455, United States;* orcid.org/0000-0002-0907-8395; Email: pierre@umn.edu

Mukesh K. Pandey − *Department of Radiology, Mayo Clinic, Rochester, Minnesota 55905, United States;* orcid.org/0000-0002-2332-5305; Email: Pandey.Mukesh@mayo.edu

Timothy R. DeGrado − *Department of Radiology, Mayo Clinic, Rochester, Minnesota 55905, United States;* orcid.org/0000-0002-0511-5398; Email: DeGrado.Timothy@mayo.edu

Authors

M. Andrey Joaqui-Joaqui − *Department of Chemistry, University of Minnesota, Minneapolis, Minnesota 55455, United States;* orcid.org/0000-0001-7446-6004

Aditya Bansal − *Department of Radiology, Mayo Clinic, Rochester, Minnesota 55905, United States;* orcid.org/0000-0001-7657-4981

Mandapati V. Ramakrishnam Raju − *Department of Chemistry, University of Minnesota, Minneapolis, Minnesota 55455, United States;* orcid.org/0000-0002-8045-5827

Fiona Armstrong-Pavlik − *Department of Chemistry, University of Minnesota, Minneapolis, Minnesota 55455, United States;* orcid.org/0000-0002-9922-5079

Ayca Dundar − *Department of Radiology, Mayo Clinic, Rochester, Minnesota 55905, United States;* orcid.org/0000-0002-3128-6801

Henry L. Wong − *Department of Medicinal Chemistry and Institute for Therapeutics Discovery & Development, University of Minnesota, Minneapolis, Minnesota 55414, United States;* orcid.org/0000-0003-1755-1485

Complete contact information is available at: https://pubs.acs.org/10.1021/acs.inorgchem.0c00975

Notes

The authors declare no competing financial interest.

ACKNOWLEDGMENTS

The authors acknowledge support from the Minnesota Partnership for Biotechnology and Genomics (Grant 17.38).

REFERENCES

(1) Wu, M.; Shu, J. Multimodal Molecular Imaging: Current Status and Future Directions. *Contrast Media Mol. Imaging* **2018**, *2018*, 1.

(2) Antoni, G.; Sörensen, J.; Hall, H. Molecular Imaging of Transporters with Positron Emission Tomography. In *Transporters as Targets for Drugs*; Napier, S., Bingham, M., Eds.; Springer: Berlin, 2009; Vol. *4*, pp 155−186.

(3) Kostelnik, T. I.; Orvig, C. Radioactive Main Group and Rare Earth Metals for Imaging and Therapy. *Chem. Rev.* **2019**, *119* (2), 902−956.

(4) Mossine, A. V.; Brooks, A. F.; Jackson, I. M.; Quesada, C. A.; Sherman, P.; Cole, E. L.; Donnelly, D. J.; Scott, P. J. H.; Shao, X. Synthesis of Diverse ^{11}C-Labeled PET Radiotracers via Direct Incorporation of [^{11}C]CO_2. *Bioconjugate Chem.* **2016**, *27* (5), 1382−1389.

(5) Pippin, A. B.; Voll, R. J.; Li, Y.; Wu, H.; Mao, H.; Goodman, M. M. Radiochemical Synthesis and Evaluation of ^{13}N-Labeled 5-Aminolevulinic Acid for PET Imaging of Gliomas. *ACS Med. Chem. Lett.* **2017**, *8* (12), 1236−1240.

(6) Horitsugi, G.; Watabe, T.; Kanai, Y.; Ikeda, H.; Kato, H.; Naka, S.; Ishibashi, M.; Matsunaga, K.; Isohashi, K.; Shimosegawa, E.; Hatazawa, J. Oxygen-15 Labeled CO_2, O_2, and CO PET in Small Animals: Evaluation Using a 3D-Mode MicroPET Scanner and Impact of Reconstruction Algorithms. *EJNMMI Res.* **2017**, *7* (1), 91.

(7) Cai, Z.; Li, S.; Pracitto, R.; Navarro, A.; Shirali, A.; Ropchan, J.; Huang, Y. Fluorine-18-Labeled Antagonist for PET Imaging of Kappa Opioid Receptors. *ACS Chem. Neurosci.* **2017**, *8* (1), 12−16.

(8) Zeglis, B. M.; Lewis, J. S. A Practical Guide to the Construction of Radiometallated Bioconjugates for Positron Emission Tomography. *Dalt. Trans.* **2011**, *40* (23), 6168−6195.

(9) Macpherson, D. S.; Fung, K.; Cook, B. E.; Francesconi, L. C.; Zeglis, B. M. A Brief Overview of Metal Complexes as Nuclear Imaging Agents. *Dalt. Trans.* **2019**, *48* (39), 14547−14565.

(10) Berry, D. J.; Ma, Y.; Ballinger, J. R.; Tavaré, R.; Koers, A.; Sunassee, K.; Zhou, T.; Nawaz, S.; Mullen, G. E. D.; Hider, R. C.; Blower, P. J. Efficient Bifunctional Gallium-68 Chelators for Positron Emission Tomography: Tris(Hydroxypyridinone) Ligands. *Chem. Commun.* **2011**, *47* (25), 7068−7070.

(11) Koukouraki, S.; Strauss, L. G.; Georgoulias, V.; Eisenhut, M.; Haberkorn, U.; Dimitrakopoulou-Strauss, A. Comparison of the Pharmacokinetics of ^{68}Ga-DOTATOC and [^{18}F]FDG in Patients with Metastatic Neuroendocrine Tumours Scheduled for ^{90}Y-DOTATOC Therapy. *Eur. J. Nucl. Med. Mol. Imaging* **2006**, *33* (10), 1115−1122.

(12) Haug, A.; Auernhammer, C. J.; Wängler, B.; Tiling, R.; Schmidt, G.; Göke, B.; Bartenstein, P.; Pöpperl, G. Intraindividual Comparison of ^{68}Ga-DOTA-TATE and ^{18}F-DOPA PET in Patients with Well-Differentiated Metastatic Neuroendocrine Tumours. *Eur. J. Nucl. Med. Mol. Imaging* **2009**, *36* (5), 765−770.

(13) Virgolini, I.; Ambrosini, V.; Bomanji, J. B.; Baum, R. P.; Fanti, S.; Gabriel, M.; Papathanasiou, N. D.; Pepe, G.; Oyen, W.; De Cristoforo, C.; Chiti, A. Procedure Guidelines for PET/CT Tumour Imaging with ^{68}Ga-DOTA-Conjugated Peptides: ^{68}Ga-DOTA-TOC, ^{68}Ga-DOTA-NOC, ^{68}Ga-DOTA-TATE. *Eur. J. Nucl. Med. Mol. Imaging* **2010**, *37* (10), 2004−2010.

(14) Prasad, V.; Ambrosini, V.; Hommann, M.; Hoersch, D.; Fanti, S.; Baum, R. P. Detection of Unknown Primary Neuroendocrine Tumours (CUP-NET) Using ^{68}Ga-DOTA-NOC Receptor PET/CT. *Eur. J. Nucl. Med. Mol. Imaging* **2010**, *37* (1), 67−77.

(15) Huo, Y.; Kang, L.; Pang, X.; Shen, H.; Yan, P.; Zhang, C.; Liao, X.; Chen, X.; Wang, R. Noninvasive PET Imaging of a Ga-68-Radiolabeled RRL-Derived Peptide in Hepatocarcinoma Murine Models. *Mol. Imaging Biol.* **2019**, *21* (2), 286−296.

(16) Velikyan, I.; Beyer, G. J.; Långström, B. Microwave-Supported Preparation of ^{68}Ga Bioconjugates with High Specific Radioactivity. *Bioconjugate Chem.* **2004**, *15* (3), 554−560.

(17) Velikyan, I.; Sundberg, Å. L.; Lindhe, Ö; Höglund, A. U.; Eriksson, O.; Werner, E.; Carlsson, J.; Bergström, M.; Långström, B.; Tolmachev, V. Preparation and Evaluation of ^{68}Ga-DOTA-hEGF for Visualization of EGFR Expression in Malignant Tumors. *J. Nucl. Med.* **2005**, *46* (11), 1881−1889.

(18) Xavier, C.; Vaneycken, I.; D'Huyvetter, M.; Heemskerk, J.; Keyaerts, M.; Vincke, C.; Devoogdt, N.; Muyldermans, S.; Lahoutte, T.; Caveliers, V. Synthesis, Preclinical Validation, Dosimetry, and Toxicity of ^{68}Ga-NOTA-Anti-HER_2 Nanobodies for iPET Imaging of HER_2 Receptor Expression in Cancer. *J. Nucl. Med.* **2013**, *54* (5), 776−784.

(19) Meyer, G. J.; Mäcke, H.; Schuhmacher, J.; Knapp, W. H.; Hofmann, M. ^{68}Ga-Labelled DOTA-Derivatised Peptide Ligands. *Eur. J. Nucl. Med. Mol. Imaging* **2004**, *31* (8), 1097−1104.

(20) Gai, Y.; Sun, L.; Lan, X.; Zeng, D.; Xiang, G.; Ma, X. Synthesis and Evaluation of New Bifunctional Chelators with Phosphonic Acid Arms for Gallium-68 Based PET Imaging in Melanoma. *Bioconjugate Chem.* **2018**, *29* (10), 3483−3494.

(21) Notni, J.; Hermann, P.; Havlíčková, J.; Kotek, J.; Kubíček, V.; Plutnar, J.; Loktionova, N.; Riss, P. J.; Rösch, F.; Lukeš, I. A Triazacyclononane-Based Bifunctional Phosphinate Ligand for the Preparation of Multimeric ^{68}Ga Tracers for Positron Emission Tomography. *Chem. - Eur. J.* **2010**, *16* (24), 7174−7185.

(22) Simecek, J.; Zemek, O.; Hermann, P.; Notni, J.; Wester, H. J. Tailored Gallium(III) Chelator NOPO: Synthesis, Characterization,

Bioconjugation, and Application in Preclinical Ga-68-PET Imaging. *Mol. Pharmaceutics* **2014**, *11* (11), 3893−3903.
(23) Ferreira, C. L.; Yapp, D. T. T.; Mandel, D.; Gill, R. K.; Boros, E.; Wong, M. Q.; Jurek, P.; Kiefer, G. E. ^{68}Ga Small Peptide Imaging: Comparison of NOTA and PCTA. *Bioconjugate Chem.* **2012**, *23* (11), 2239−2246.
(24) Fazaeli, Y.; Jalilian, A. R.; Amini, M. M.; Ardaneh, K.; Rahiminejad, A.; Bolourinovin, F.; Moradkhani, S.; Majdabadi, A. Development of a ^{68}Ga-Fluorinated Porphyrin Complex as a Possible PET Imaging Agent. *Nucl. Med. Mol. Imaging* **2012**, *46* (1), 20−26.
(25) Wagner, S. J.; Welch, M. J. Gallium-68 Labelling of Albumin and Albumin Microspheres. *J. Nucl. Med.* **1979**, *20* (5), 428−433.
(26) Prinsen, K.; Li, J.; Vanbilloen, H.; Vermaelen, P.; Devos, E.; Mortelmans, L.; Bormans, G.; Ni, Y.; Verbruggen, A. Development and Evaluation of a ^{68}Ga Labeled Pamoic Acid Derivative for in Vivo Visualization of Necrosis Using Positron Emission Tomography. *Bioorg. Med. Chem.* **2010**, *18* (14), 5274−5281.
(27) Smith-Jones, P. M.; Stolz, B.; Bruns, C.; Albert, R.; Reist, H. W.; Fridrich, R.; Macke, H. R. Gallium-67/Gallium-68-[DFO]-Octreotide - A Potential Radiopharmaceutical for PET Imaging of Somatostatin Receptor-Positive Tumors: Synthesis and Radiolabeling in Vitro and Preliminary in Vivo Studies. *J. Nucl. Med.* **1994**, *35* (2), 317−325.
(28) Satpati, D.; Sharma, R.; Kumar, C.; Sarma, H. D.; Dash, A. ^{68}Ga-Chelation and Comparative Evaluation of N,N′-Bis-[2-Hydroxy-5-(Carboxyethyl)Benzyl]Ethylenediamine-N,N′-Diacetic Acid (HBED-CC) Conjugated NGR and RGD Peptides as Tumor Targeted Molecular Imaging Probes. *MedChemComm* **2017**, *8* (3), 673−679.
(29) Eder, M.; Neels, O.; Müller, M.; Bauder-Wüst, U.; Remde, Y.; Schäfer, M.; Hennrich, U.; Eisenhut, M.; Afshar-Oromieh, A.; Haberkorn, U.; Kopka, K. Novel Preclinical and Radiopharmaceutical Aspects of [^{68}Ga]Ga-PSMA-HBED-CC: A New PET Tracer for Imaging of Prostate Cancer. *Pharmaceuticals* **2014**, *7* (7), 779−796.
(30) Maurer, T.; Eiber, M.; Schwaiger, M.; Gschwend, J. E. Current Use of PSMA-PET in Prostate Cancer Management. *Nat. Rev. Urol.* **2016**, *13* (4), 226−235.
(31) Boros, E.; Ferreira, C. L.; Cawthray, J. F.; Price, E. W.; Patrick, B. O.; Wester, D. W.; Adam, M. J.; Orvig, C. Acyclic Chelate with Ideal Properties for ^{68}Ga PET Imaging Agent Elaboration. *J. Am. Chem. Soc.* **2010**, *132* (44), 15726−15733.
(32) Waldron, B. P.; Parker, D.; Burchardt, C.; Yufit, D. S.; Zimny, M.; Roesch, F. Structure and Stability of Hexadentate Complexes of Ligands Based on AAZTA for Efficient PET Labelling with Gallium-68. *Chem. Commun.* **2013**, *49* (6), 579−581.
(33) Seemann, J.; Waldron, B. P.; Roesch, F.; Parker, D. Approaching 'Kit-Type' Labelling with ^{68}Ga: The DATA Chelators. *ChemMedChem* **2015**, *10* (6), 1019−1026.
(34) Farkas, E.; Vágner, A.; Negri, R.; Lattuada, L.; Tóth, I.; Colombo, V.; Esteban-Gómez, D.; Platas-Iglesias, C.; Notni, J.; Baranyai, Z.; Giovenzana, G. B. PIDAZTA: Structurally Constrained Chelators for the Efficient Formation of Stable Gallium-68 Complexes at Physiological pH. *Chem. - Eur. J.* **2019**, *25* (45), 10698−10709.
(35) Wang, X.; Jaraquemada-Peláez, M. D. G.; Cao, Y.; Pan, J.; Lin, K. S.; Patrick, B. O.; Orvig, C. H_2hox: Dual-Channel Oxine-Derived Acyclic Chelating Ligand for ^{68}Ga Radiopharmaceuticals. *Inorg. Chem.* **2019**, *58* (4), 2275−2285.
(36) Chitambar, C. R. Gallium and Its Competing Roles with Iron in Biological Systems. *Biochim. Biophys. Acta, Mol. Cell Res.* **2016**, *1863* (8), 2044−2053.
(37) Petrik, M.; Zhai, C. Y.; Haas, H.; Decristoforo, C. Siderophores for Molecular Imaging Applications. *Clin. Transl. Imaging* **2017**, *5* (1), 15−27.
(38) Stolz, B.; Smith-Jones, P. M.; Albert, R.; Reist, H.; Macke, H.; Bruns, C. Biological Characterisation of [^{67}Ga] or [^{68}Ga] Labelled DFO-Octreotide (SDZ 216−927) for PET Studies of Somatostatin Receptor Positive Tumors. *Horm. Metab. Res.* **1994**, *26* (10), 453−459.
(39) Eisenwiener, K. P.; Prata, M. I. M.; Buschmann, I.; Zhang, H. W.; Santos, A. C.; Wenger, S.; Reubi, J. C.; Mäcke, H. R. NODAGATOC, a New Chelator-Coupled Somatostatin Analogue Labeled with [$^{67/68}$Ga] and [^{111}In] for SPECT, PET, and Targeted Therapeutic Applications of Somatostatin Receptor (hsst2) Expressing Tumors. *Bioconjugate Chem.* **2002**, *13* (3), 530−541.
(40) Govindan, S. V.; Michel, R. B.; Griffiths, G. L.; Goldenberg, D. M.; Mattes, M. J. Deferoxamine as a Chelator for ^{67}Ga in the Preparation of Antibody Conjugates. *Nucl. Med. Biol.* **2005**, *32* (5), 513−519.
(41) Caraco', C.; Aloj, L.; Eckelman, W. C. The Gallium−Deferoxamine Complex: Stability with Different Deferoxamine Concentrations and Incubation Conditions. *Appl. Radiat. Isot.* **1998**, *49* (12), 1477−1479.
(42) Ryser, J.-E.; Rose, K.; Jones, R.; Pelegrin, A.; Donath, A.; Egeli, R.; Smith, A.; Offord, R. E. Elimination of Free Radionuclide by a Chelating Agent Improves Tumor-to-Nontumor Ratios Following Radioimmunotargeting with Antibody Labeled with ^{67}Ga. *Nucl. Med. Biol.* **1998**, *25* (3), 261−265.
(43) Petrik, M.; Umlaufova, E.; Raclavsky, V.; Palyzova, A.; Havlicek, V.; Haas, H.; Novy, Z.; Dolezal, D.; Hajduch, M.; Decristoforo, C. Imaging of Pseudomonas Aeruginosa Infection with Ga-68 Labelled Pyoverdine for Positron Emission Tomography. *Sci. Rep.* **2018**, *8* (1), 15689.
(44) Harris, W. R.; Carrano, C. J.; Cooper, S. R.; Sofen, S. R.; Avdeef, A. E.; McArdle, J. V.; Raymond, K. N. Coordination Chemistry of Microbial Iron Transport Compounds. 19. Stability Constants and Electrochemical Behavior of Ferric Enterobactin and Model Complexes. *J. Am. Chem. Soc.* **1979**, *101* (20), 6097−6104.
(45) Ecker, D. J.; Matzanke, B. F.; Raymond, K. N. Recognition and Transport of Ferric Enterobactin in Escherichia Coli. *J. Bacteriol.* **1986**, *167* (2), 666−673.
(46) Loomis, L. D.; Raymond, K. N. Solution Equilibria of Enterobactin and Metal-Enterobactin Complexes. *Inorg. Chem.* **1991**, *30* (5), 906−911.
(47) Thulasiraman, P.; Newton, S. M. C.; Xu, J. D.; Raymond, K. N.; Mai, C.; Hall, A.; Montague, M. A.; Klebba, P. E. Selectivity of Ferric Enterobactin Binding and Cooperativity of Transport in Gram-Negative Bacteria. *J. Bacteriol.* **1998**, *180* (24), 6689−6696.
(48) Raymond, K. N.; Dertz, E. A.; Kim, S. S. Enterobactin: An Archetype for Microbial Iron Transport. *Proc. Natl. Acad. Sci. U. S. A.* **2003**, *100* (7), 3584−3588.
(49) D'Hardemare, A. D. M.; Torelli, S.; Serratrice, G.; Pierre, J. L. Design of Iron Chelators: Syntheses and Iron (III) Complexing Abilities of Tripodal Tris-Bidentate Ligands. *BioMetals* **2006**, *19* (4), 349−366.
(50) Rodgers, S. J.; Lee, C. W.; Ng, C. Y.; Raymond, K. N. Ferric Ion Sequestering Agents. 15. Synthesis, Solution Chemistry, and Electrochemistry of a New Cationic Analogue of Enterobactin. *Inorg. Chem.* **1987**, *26* (10), 1622−1625.
(51) Gardner, R. A.; Kinkade, R.; Wang, C.; Phanstiel. Total Synthesis of Petrobactin and Its Homologues as Potential Growth Stimuli for Marinobacter Hydrocarbonoclasticus, an Oil-Degrading Bacteria. *J. Org. Chem.* **2004**, *69* (10), 3530−3537.
(52) Maier, G. P.; Bernt, C. M.; Butler, A. Catechol Oxidation: Considerations in the Design of Wet Adhesive Materials. *Biomater. Sci.* **2018**, *6* (2), 332−339.
(53) Yu, J.; Wei, W.; Danner, E.; Ashley, R. K.; Israelachvili, J. N.; Waite, J. H. Mussel Protein Adhesion Depends on Interprotein Thiol-Mediated Redox Modulation. *Nat. Chem. Biol.* **2011**, *7* (9), 588−590.
(54) Allred, B. E.; Correnti, C.; Clifton, M. C.; Strong, R. K.; Raymond, K. N. Siderocalin Outwits the Coordination Chemistry of Vibriobactin, a Siderophore of Vibrio Cholerae. *ACS Chem. Biol.* **2013**, *8* (9), 1882−1887.
(55) Dertz, E. A.; Xu, J.; Raymond, K. N. Tren-Based Analogues of Bacillibactin: Structure and Stability. *Inorg. Chem.* **2006**, *45* (14), 5465−5478.
(56) Pierre, V. C.; Melchior, M.; Doble, D. M. J.; Raymond, K. N. Toward Optimized High-Relaxivity MRI Agents: Thermodynamic

Selectivity of Hydroxypyridonate/Catecholate Ligands. *Inorg. Chem.* **2004**, *43* (26), 8520−8525.
(57) Pierre, V. C.; Botta, M.; Aime, S.; Raymond, K. N. Substituent Effects on Gd(III)-Based MRI Contrast Agents: Optimizing the Stability and Selectivity of the Complex and the Number of Coordinated Water Molecules. *Inorg. Chem.* **2006**, *45* (20), 8355−8364.
(58) Tsionou, M. I.; Knapp, C. E.; Foley, C. A.; Munteanu, C. R.; Cakebread, A.; Imberti, C.; Eykyn, T. R.; Young, J. D.; Paterson, B. M.; Blower, P. J.; Ma, M. T. Comparison of Macrocyclic and Acyclic Chelators for Gallium-68 Radiolabelling. *RSC Adv.* **2017**, *7* (78), 49586−49599.
(59) O'Sullivan, B.; Doble, D. M. J.; Thompson, M. K.; Siering, C.; Xu, J.; Botta, M.; Aime, S.; Raymond, K. N. The Effect of Ligand Scaffold Size on the Stability of Tripodal Hydroxypyridonate Gadolinium Complexes. *Inorg. Chem.* **2003**, *42* (8), 2577−2583.
(60) Raymond, K. N.; Pierre, V. C. Next Generation, High Relaxivity Gadolinium MRI Agents. *Bioconjugate Chem.* **2005**, *16* (1), 3−8.
(61) Huang, S.-Y.; Qian, M.; Pierre, V. C. The Ligand Cap Affects the Coordination Number but Not Necessarily the Affinity for Anions of Tris-Bidentate Europium Complexes. *Inorg. Chem.* **2020**, *59*, 4096−4108.
(62) Ramakrishnam Raju, M. V.; Wilharm, R. K.; Dresel, M. J.; McGreal, M. E.; Mansergh, J. P.; Marting, S. T.; Goodpaster, J. D.; Pierre, V. C. The Stability of the Complex and the Basicity of the Anion Impact the Selectivity and Affinity of Tripodal Gadolinium Complexes for Anions. *Inorg. Chem.* **2019**, *58* (22), 15189−15201.
(63) Sun, Y.; Anderson, C. J.; Pajeau, T. S.; Reichert, D. E.; Hancock, R. D.; Motekaitis, R. J.; Martell, A. E.; Welch, M. J. Indium(III) and Gallium(III) Complexes of Bis(Aminoethanethiol) Ligands with Different Denticities: Stabilities, Molecular Modeling, and in Vivo Behavior. *J. Med. Chem.* **1996**, *39* (2), 458−470.
(64) Jarjayes, O.; Mortini, F.; Du Moulinet D'Hardemare, A.; Philouze, C.; Serratrice, G. Tuning PGa with Chelating Agents Related to (*o*-Hydroxybenzyl)Iminodiacetic Acid. *Eur. J. Inorg. Chem.* **2005**, *2005* (21), 4417−4424.
(65) Ametamey, S. M.; Honer, M.; Schubiger, P. A. Molecular Imaging with PET. *Chem. Rev.* **2008**, *108* (5), 1501−1516.
(66) Pandey, M. K.; Byrne, J. F.; Jiang, H.; Packard, A. B.; DeGrado, T. R. Cyclotron Production of ^{68}Ga via the ^{68}Zn(p,n)^{68}Ga Reaction in Aqueous Solution. *Am. J. Nucl. Med. Mol. Imaging* **2014**, *4* (4), 303−310.
(67) Pandey, M. K.; Byrne, J. F.; Schlasner, K. N.; Schmit, N. R.; DeGrado, T. R. Cyclotron Production of ^{68}Ga in a Liquid Target: Effects of Solution Composition and Irradiation Parameters. *Nucl. Med. Biol.* **2019**, *74*−*75* (2019), 49−55.
(68) Bardal, S. K.; Waechter, J. E.; Martin, D. S. Chapter 2 - Pharmacokinetics. In *Applied Pharmacology*; Bardal, S. K., Waechter, J. E., Martin, D. S. B. T.-A. P., Eds.; Elsevier: Philadelphia, 2011; pp 17−34.
(69) Pandey, M. K.; Bansal, A.; Engelbrecht, H. P.; Byrne, J. F.; Packard, A. B.; DeGrado, T. R. Improved Production and Processing of ^{89}Zr Using a Solution Target. *Nucl. Med. Biol.* **2016**, *43* (1), 97−100.

https://dx.doi.org/10.1021/acs.inorgchem.0c00975
Inorg. Chem. XXXX, XXX, XXX−XXX